

# Applications of Conditional Nonlinear Optimal Perturbations to the Studies of ENSO and THC

Mu Mu

Key Laboratory of Ocean Circulation and Wave,  
Institute of Oceanology, Chinese Academy of Sciences

E-mail: [mumu@qdio.ac.cn](mailto:mumu@qdio.ac.cn)

# Outline

- 1 Introduction :Predictability and Conditional Nonlinear Optimal Perturbation (CNOP)
- 2 "Spring predictability barrier" of El Niño prediction
- 3 Decadal Variabilities of THC
4. Discussion

**Predictability is a fundamental issue in  
Weather and climate prediction**

**Uncertainties of prediction comes from :**

**initial errors and model errors (particularly, the  
parameter errors in the numerical models).**

**Question:**

**What kind of initial or/and parameter errors  
result in significant forecast uncertainties?**

# Linear singular vector (LSV)

Lorenz ?

$$\begin{cases} \frac{\partial(\delta w)}{\partial t} + \frac{\partial F}{\partial w} \Big|_{w=U} (w, x, t; P) \delta w = 0 \\ \delta w \Big|_{t=0} = \delta w_0 \end{cases}$$

$$\delta w(x, T) = M_T(\delta w_0)$$

$M_T$  (linear) propagator

$\delta w_0^*$  is LSV if and only if ,

$$J(\delta w_0^*) = \max_{\delta w_0} J(\delta w_0),$$

$$\text{where } J(\delta w_0) = \frac{\| M_T(P)(\delta w_0) \|}{\| \delta w_0 \|}$$

# Conditional nonlinear optimal perturbation (CNOP)

$$\begin{cases} \frac{\partial U}{\partial t} = F(U, P) \\ U|_{t=0} = U_0 \end{cases} \quad \begin{array}{l} P \text{ is parameter; } p \text{ is its perturbation} \\ U \text{ is state vector; } u_0 \text{ is initial perturbation} \end{array}$$

$$U(\tau) + u(u_0, p; \tau) = M_\tau(P + p)(U_0 + u_0)$$

$u(u_0, p; \tau)$  is the departure from the basic state caused by the initial and parametric perturbations

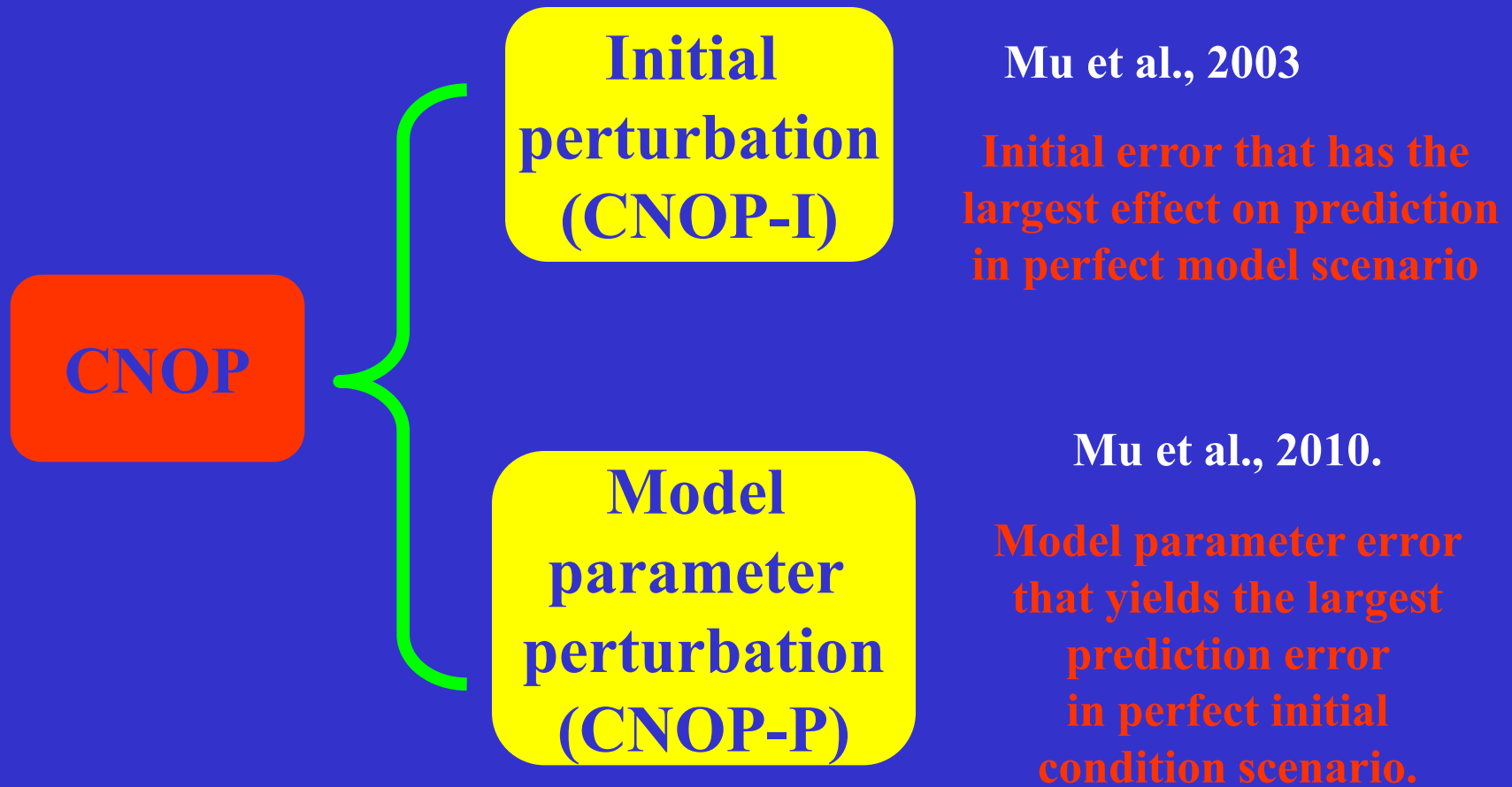
## Objective function

$$J(u_{0\delta}; p_\sigma) = \max_{u_0 \in C_\delta, p' \in C_\sigma} \|M_\tau(P + p)(U_0 + u_0) - M_\tau(P)(U_0)\|$$

**CNOP,  $(u_{0\delta}; p_\sigma)$ , is the optimal combined mode of initial and parametric perturbations**

*(Mu et al., 2010.)*

# Two special cases of CNOP



## CNOP-I:

A natural generalization of LSV in nonlinear regime

### Objective function

$$J(u_{0\delta}) = \max_{\|u_0\| \leq \delta} \| M_T(P)(U_0 + u_0) - M_T(P)(U_0) \|$$

$u_{0\delta}$  **CNOP-I**

$\| u_0 \| \leq \delta$  **Constraint condition**

## Physics of CNOP-I

```
graph TD; A[Physics of CNOP-I] --> B[Optimal precursor of a weather or climate event]; A --> C[Optimally growing initial errors];
```

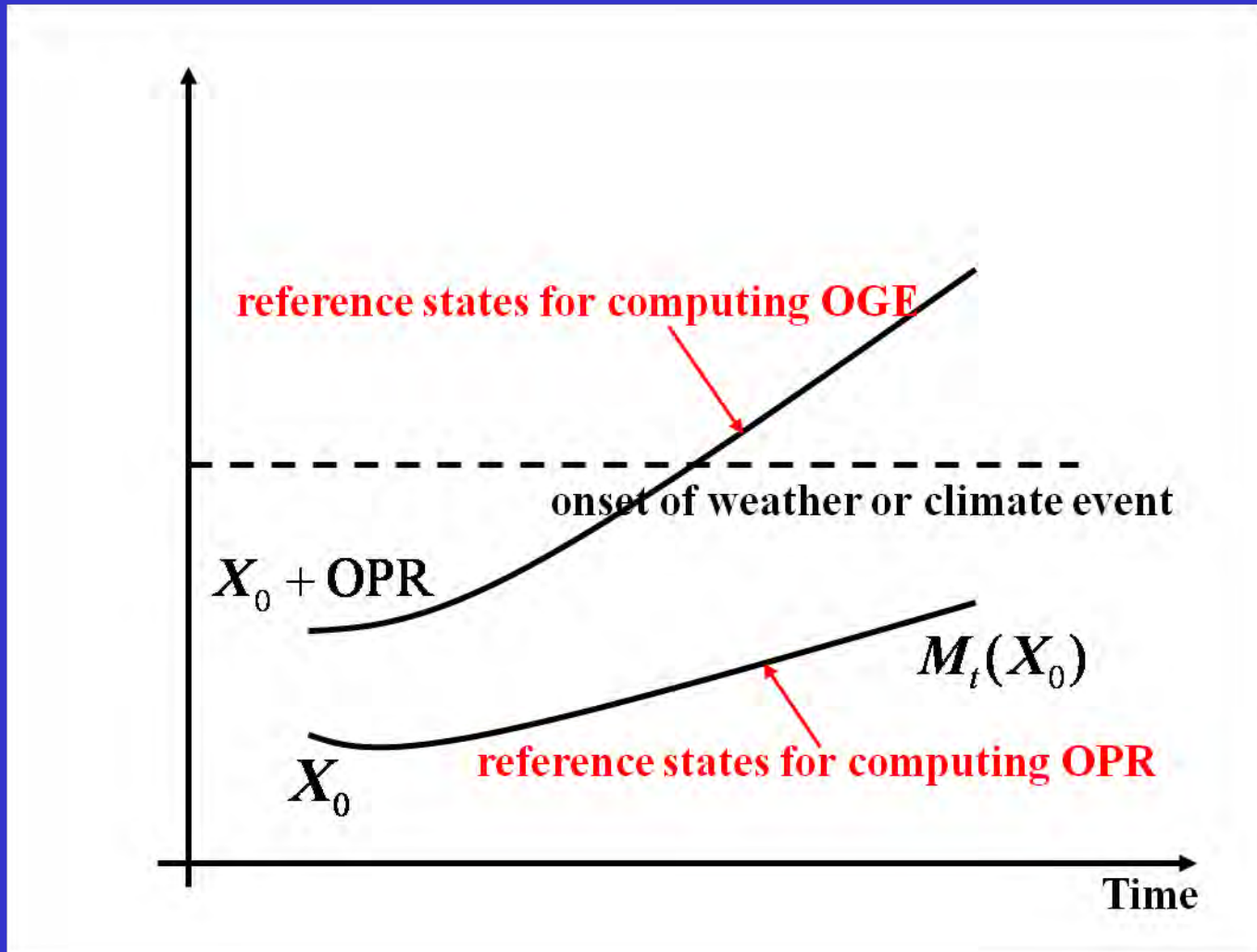
**Optimal precursor  
of a weather or climate  
event**

*Mu et al., 2003*  
*Duan et al., 2004*

**Optimally growing  
initial errors**

*Mu et al., 2003*  
*Mu et al., 2007*

# Reference states for computing OPR and OGE



# Applications of CNOP-I to the studies of weather and climate predictabilities

Optimal precursors & nonlinear behavior of ENSO decaying phase; (JGR; AR; Duan and Mu)

Spring predictability barrier for ENSO (JGR; GRL; AAS; Mu et al.; Duan et al.)

Decadal variability and ENSO asymmetry (JGR; Duan and Mu)

THC (JPO; JGR; Mu, Sun, Wu)

**CNOP-I**

Blocking (JAS; Mu and Jiang)

Double-gyre ocean circulation (NPG; Terwisscha Van Scheltinga and Dijkstra)

Target observation for tropical cyclone (Mu et al. 2009, MWR)

Ensemble forecast (Sci. Chin.; Mu and Jiang)

## CNOP-P:

$$J(p_\delta) = \max_{\|p\| \leq \delta} \| M_T(P + p)(U_0) - M_T(P)(U_0) \|$$

$\| p \| \leq \delta$  : constraint condition of parameters

$M_T$  : nonlinear propagator

$p_\delta$  : CNOP-P

### Physics of CNOP-P

CNOP-P represents the model parameter error that has the largest effect on prediction and describes a kind of important model error.

# Computation of CNOPs

**Computation of CNOP  
CNOP-I and CNOP-P**

**Constrained  
optimization  
problem**

**High-efficient  
optimization algorithm**



**Constrained **minimization** problem**  
**Algorithms: SPG2; L-BFGS; etc.**

**Computation of CNOP  
CNOP-I and CNOP-P**



**Gradients  
( adjoint ,ensemble )**

# Model and CPU time for calculating CNOP

## Adjoint method

MM5:  $\sim 10^5$

WRF:  $\sim 10^6$

ZC model:  $\sim 10^3$

## Implicit model method

Shallow water model:  $\sim 10^5$

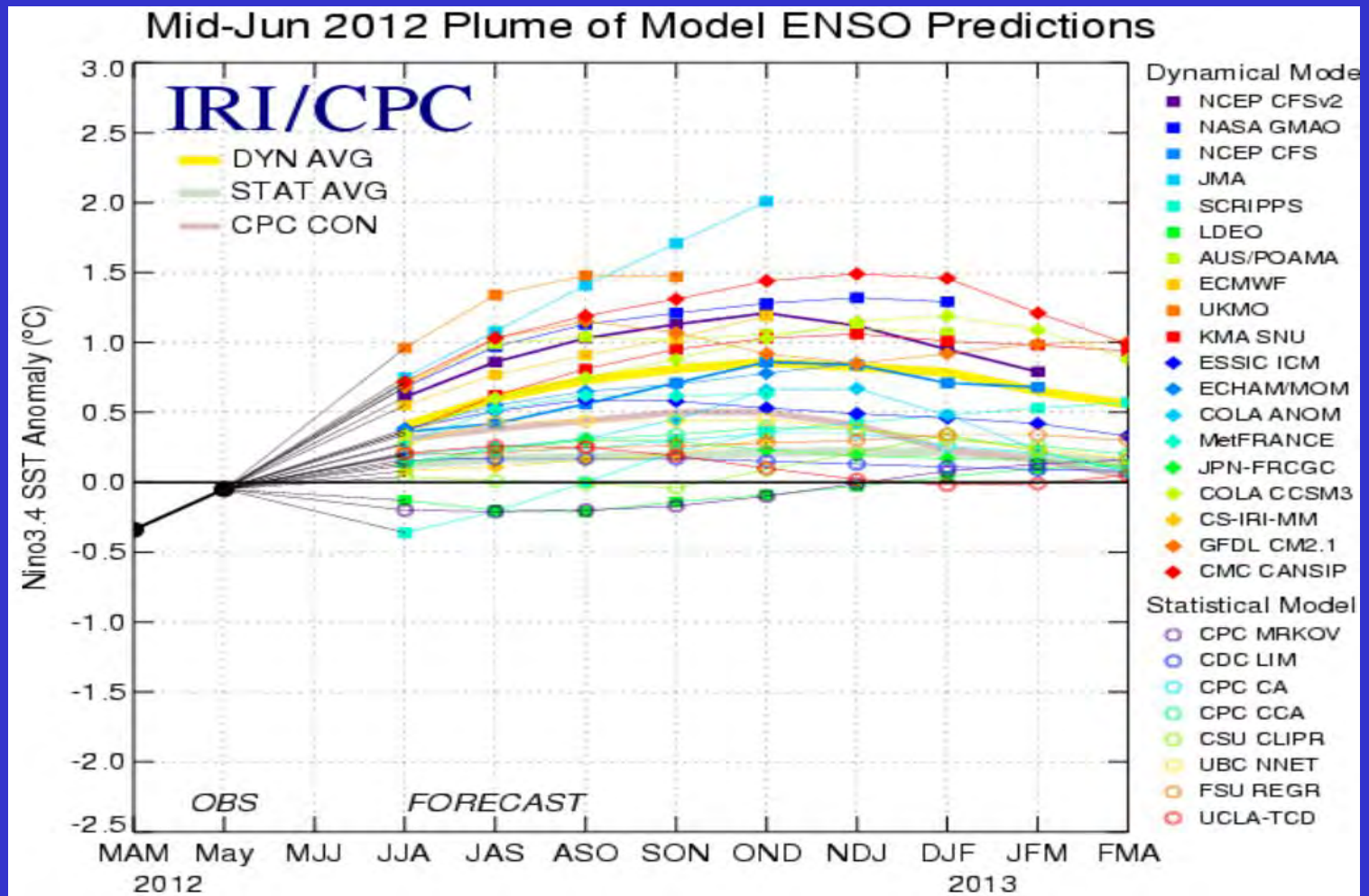
THC model:  $\sim 10^4$

## Ensemble method

GRAPES:  $\sim 10^5$

## **2. Studies of “spring predictability barrier” for El Nino events**

# Current status of ENSO forecast skill



12 dynamical models and 8 statistical models

**ENSO predictions are still of large uncertainties!**

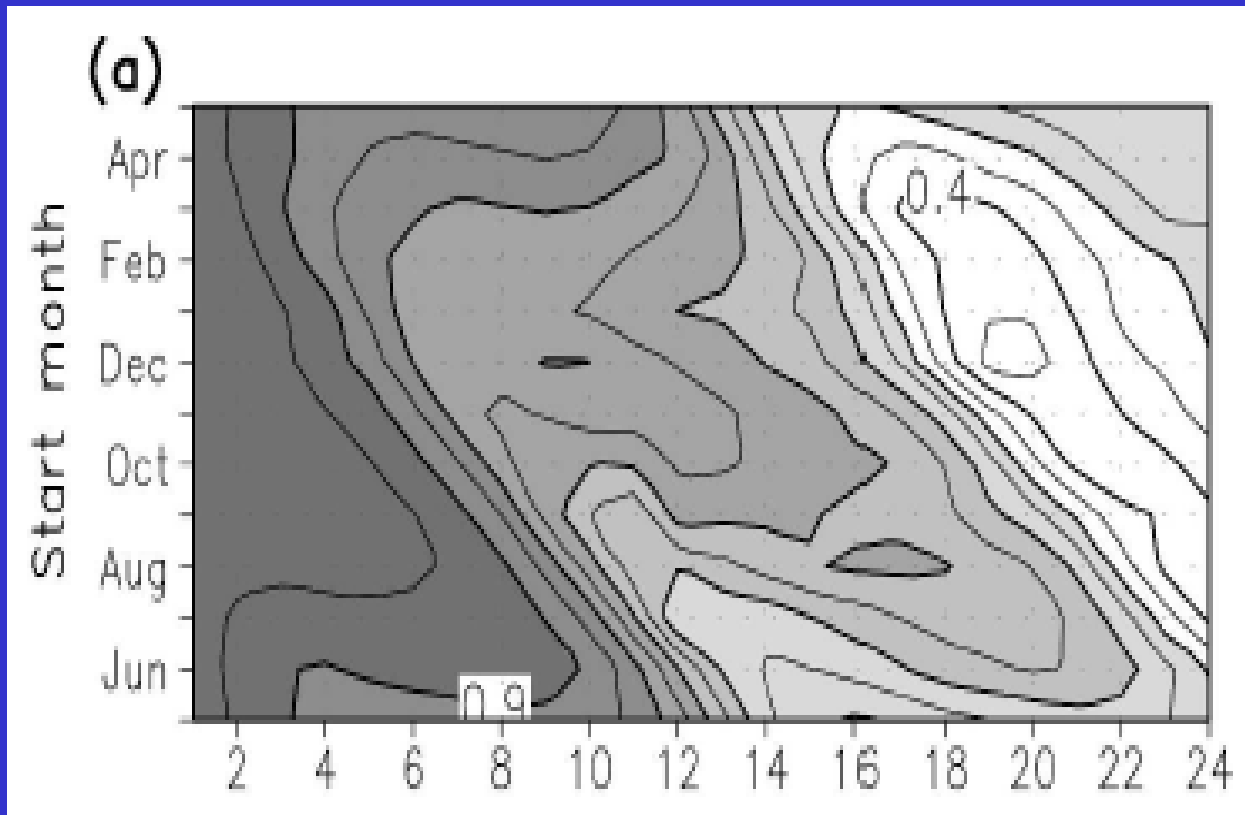
**“Spring predictability barrier” (SPB):**

**a well-known characteristic of ENSO forecast;  
severely affect ENSO forecast.**

**What is the SPB?**

## *A significant SPB:*

*During the boreal spring time, the ENSO forecast skill of most of the climate models (but not all) declines dramatically (Webster and Yang, 1992; Latif et al., 1994).*



*Luo, J.-J., S. Masson, S. Behera, and T. Yamagata 2008: Extended ENSO predictions using a fully coupled ocean-atmosphere model. J. Climate, 21(1), 84-93.*

## **(ii) Properties of the SPB**

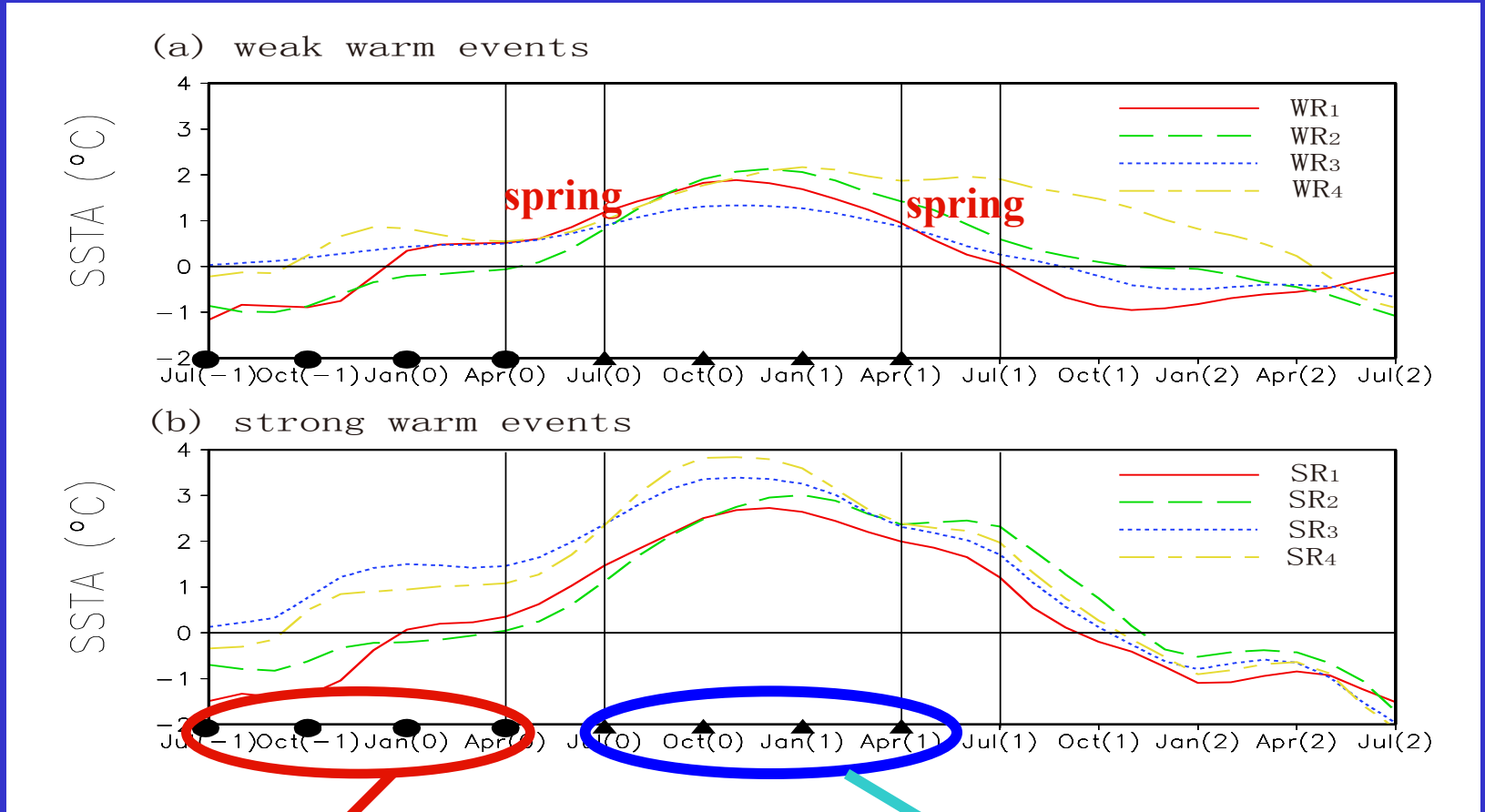
**Samelson and Tziperman [2001]:  
the SPB is an inherent characteristic of ENSO forecast;**

**However,**

**Chen et al. [1995, 2004]: *the SPB can be reduced through improving initialization.***

# 2.1. Season-dependent predictability caused by initial errors

Reference States: El Nino events in Zebiak-Cane model



Growth-phase prediction

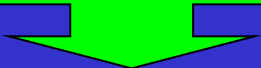
Decaying-phase prediction

# Seasonal growth rates of prediction error caused by CNOP-I errors

## Growth-phase predictions

Start month: July in year (-1)

Largest Prediction errors  
of Niño-3 SSTA



	JAS	OND	JFM	AMJ	$E_{Ni\tilde{no}-3}$
WR <sub>1</sub>	2.171	1.109	3.564	4.510	-1.796
WR <sub>2</sub>	1.338	2.496	-0.941	4.096	1.422
WR <sub>3</sub>	2.107	2.850	1.530	3.017	1.781
WR <sub>4</sub>	2.588	3.166	1.811	2.678	1.826
SR <sub>1</sub>	1.819	1.028	3.133	4.774	-1.794
SR <sub>2</sub>	1.050	0.318	1.535	5.321	-1.603
SR <sub>3</sub>	2.206	3.014	3.420	5.577	-2.242
SR <sub>4</sub>	2.552	3.410	0.163	-0.683	0.802

**Start month: October in year (-1)**

**Largest Prediction errors  
of Nino-3 SSTA**



	OND	JFM	AMJ	JAS	E-Nino3
$WR^1_{Jan}$	2.397	1.888	3.678	3.620	2.008
$WR^1_{Apr}$	0.933	-0.045	3.219	4.973	1.639
$WR^1_{Jul}$	1.415	1.615	4.281	4.327	2.207
$WR^1_{Oct}$	0.985	1.392	3.294	2.783	1.496
$SR^1_{Jan}$	1.525	2.018	8.187	5.176	-2.880
$SR^1_{Apr}$	1.103	1.342	5.315	6.476	-2.693
$SR^1_{Jul}$	1.710	2.186	5.722	3.177	-2.110
$SR^1_{Oct}$	1.776	1.678	5.757	4.901	-2.337



**Growth phase**

Start month: January in year (0)

Largest Prediction errors  
of Niño-3 SSTA

	JFM	AMJ	JAS	OND	$E_{Ni\tilde{no}-3}$
WR <sub>1</sub>	1.445	2.882	4.995	0.678	1.740
WR <sub>2</sub>	1.132	3.409	5.358	4.352	-2.573
WR <sub>3</sub>	1.010	4.242	5.507	1.396	2.218
WR <sub>4</sub>	0.902	3.945	7.017	3.103	-2.762
SR <sub>1</sub>	1.301	5.739	8.716	1.802	-3.147
SR <sub>2</sub>	1.348	3.922	7.685	4.808	-3.316
SR <sub>3</sub>	1.629	4.488	7.511	2.879	-3.005
SR <sub>4</sub>	1.844	4.504	7.724	1.837	-2.694

Growth phase

**Growth-phase predictions: CNOP-type initial errors have a obvious season-dependent evolution of prediction errors and cause the largest prediction errors.**

**The decaying-phase predictions have similar results.**

**CNOP-type initial errors can cause a significant SPB for El Nino events**

### 3. Season-dependent predictability caused by model errors?

Main experiential parameters in the ZC model and their physics and given values

Atmospheric equation

Temperature equation

Subsurface temperature

Wind forcing

Parameter	Physical Meaning	Value
$\alpha$	Controlling strength of SST-related component of atmospheric heating	1.6
$\beta$	Controlling strength of convergence feedback portion of atmospheric heating	0.75
$\varepsilon$	Atmospheric friction parameter	0.3
$\eta$	Affecting surface heat flux(a linear damping on SSTA)	0.98
T1	$h > 0$ , affecting amplitude of subsurface temperature anomaly for positive h perturbations	28.0
b1	$h > 0$ , affecting the nonlinearity of subsurface temperature anomaly for positive h perturbations	1.25
T2	$h < 0$ , affecting amplitude of subsurface temperature anomaly for negative h perturbations	-40.0
b2	$h < 0$ , affecting the nonlinearity of subsurface temperature anomaly for negative h perturbations	3.0
$\sigma$	Controlling strength of wind stress	0.0329

**CNOP-P causes the largest prediction error.**

**Can the CNOP-P error superimposed on these parameters cause a significant SPB?**

**(1) Seasonal growth rate of the prediction error caused by CNOP-P errors**

**(2) The prediction error of Nino-3 SSTA caused by CNOP-P errors**

**Small  
prediction  
errors**

## Growth-phase predictions

Start month: July in year (-1)

El Nino	JAS	OND	JFM	AMJ	$E_{Ni\tilde{n}o-3}$
WR <sub>1</sub>	0.098	0.024	0.082	<i>0.182</i>	0.002
WR <sub>2</sub>	0.533	0.187	1.204	<i>0.433</i>	0.242
WR <sub>3</sub>	0.01	0.083	0.099	<i>0.122</i>	0.037
WR <sub>4</sub>	0.245	<i>0.301</i>	0.096	0.062	0.104
SR <sub>1</sub>	0.393	0.383	0.432	<i>0.371</i>	0.164
SR <sub>2</sub>	0.354	0.153	0.26	<i>0.669</i>	0.262
SR <sub>3</sub>	0.07	0.154	0.182	<i>0.446</i>	0.158
SR <sub>4</sub>	0.106	0.12	0.103	<i>0.276</i>	-0.095

Small prediction errors

## Start month: October in year (-1)

El Nino	OND	JFM	AMJ	JAS	$E_{Ni\tilde{n}o-3}$
WR <sub>1</sub>	0.117	0.187	0.287	<b>0.313</b>	0.067
WR <sub>2</sub>	0.179	0.175	<b>0.232</b>	0.171	0.028
WR <sub>3</sub>	0.027	0.049	0.136	<b>0.247</b>	0.085
WR <sub>4</sub>	0.04	0.061	0.182	<b>0.303</b>	0.111
SR <sub>1</sub>	0.183	0.286	0.811	<b>0.877</b>	-0.213
SR <sub>2</sub>	0.054	0.008	0.257	<b>0.783</b>	-0.178
SR <sub>3</sub>	0.127	0.145	0.437	<b>0.691</b>	-0.253
SR <sub>4</sub>	0.054	0.07	0.255	<b>0.734</b>	-0.143

Small prediction errors

Start month: January in year (0)

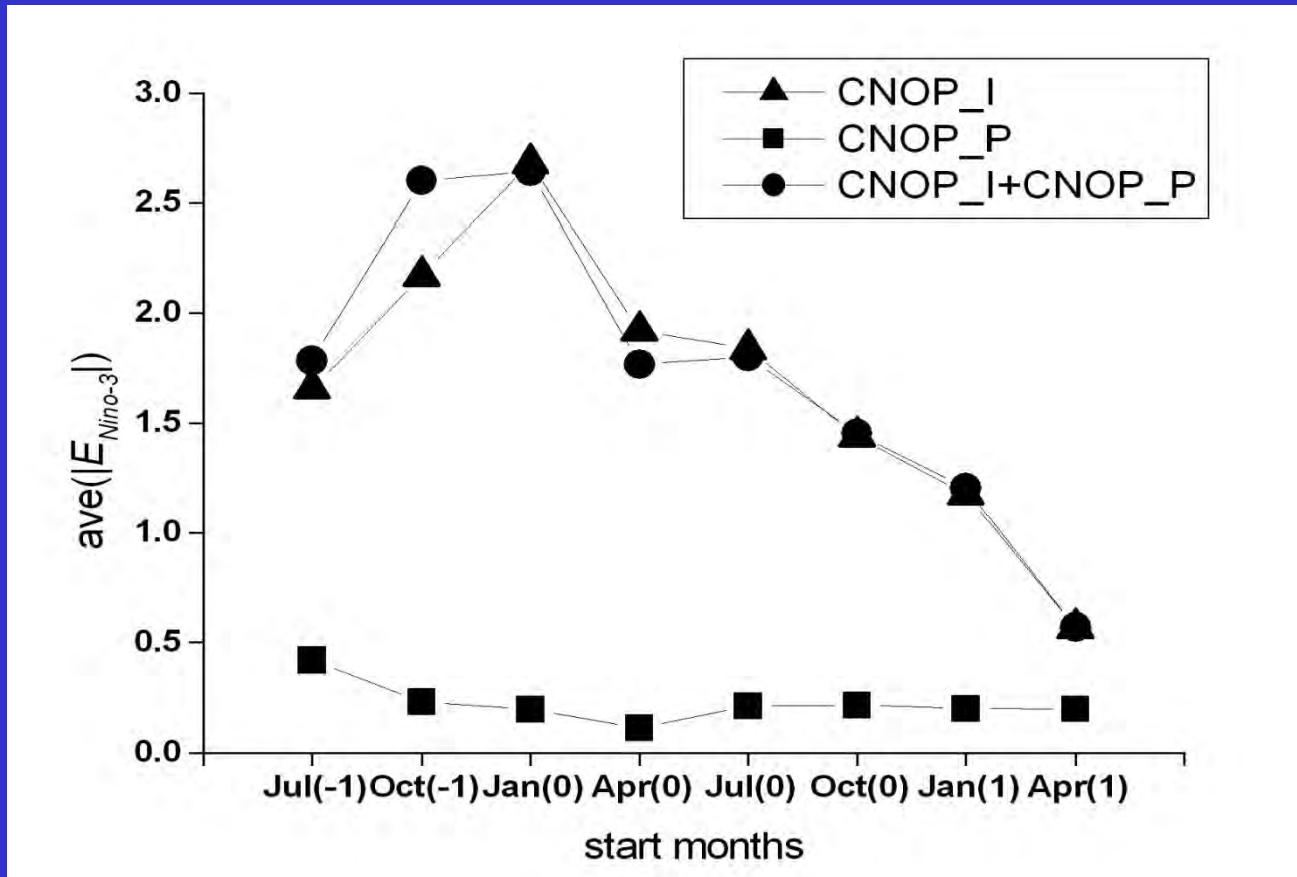
El Nino	JFM	AMJ	JAS	OND	$E_{Ni\tilde{n}o-3}$
WR <sub>1</sub>	0.055	0.23	0.463	0.416	0.203
WR <sub>2</sub>	0.032	0.165	0.307	0.258	-0.135
WR <sub>3</sub>	0.034	0.122	0.263	0.234	0.121
WR <sub>4</sub>	0.049	0.107	0.304	0.374	0.158
SR <sub>1</sub>	0.028	0.203	0.618	0.739	0.29
SR <sub>2</sub>	0.023	0.32	0.431	0.36	0.187
SR <sub>3</sub>	0.121	0.451	0.873	0.497	0.33
SR <sub>4</sub>	0.075	0.265	0.643	0.165	-0.156

**For the growth-phase predictions, the CNOP-P errors have obvious season-dependent evolutions, but the error growth rate in each season are very small and the prediction errors caused by CNOP-P errors are negligible.**

**The decaying-phase predictions have similar results**

**CNOP-P does not cause a significant SPB and could not be the dominant source of the uncertainties that cause a significant SPB.**

# Prediction errors caused by the CNOP-I, CNOP-P, and the combined mode of them



The prediction errors caused by CNOP-I errors are trivially different from those caused by the combined mode of CNOP-I and CNOP-P.

The parameter errors in the ZC model may have a negligible effect on ENSO prediction.

**CNOP-I errors:  
a significant SPB**

**CNOP-P errors  
Fail to cause  
a significant SPB**

**The combined mode  
of CNOP-I and CNOP-P  
a significant SPB**

**A significant SPB:  
related to initial error**



**Initial error may be the  
dominant source of the  
uncertainties that cause a  
significant SPB**

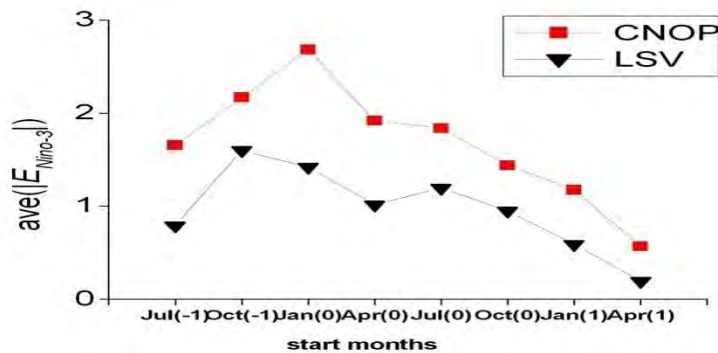
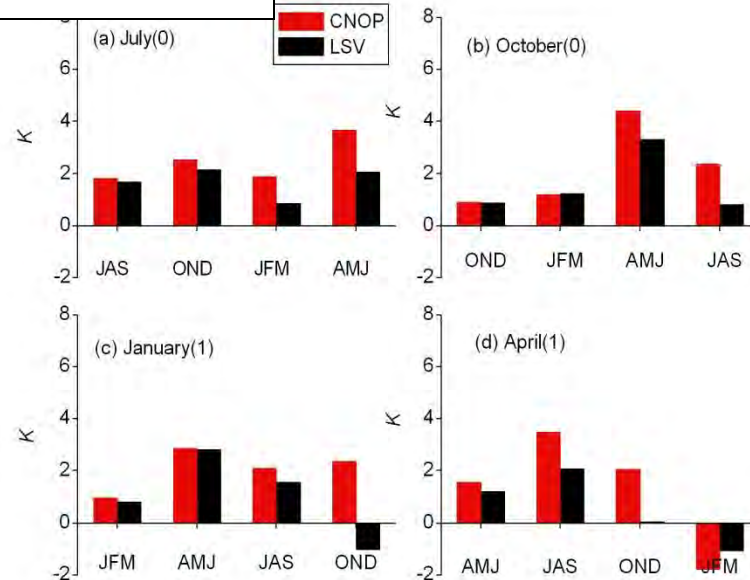
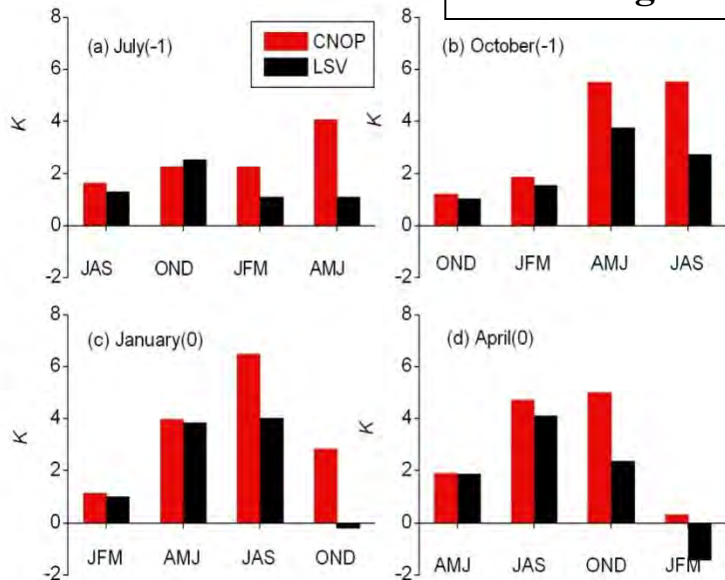
**CNOP-I error causes the largest prediction errors and has an obvious season-dependent evolution, being most likely to cause a significant SPB!**

# 4. Dependence of SPB on initial error patterns

## Growth-phase predictions

## Decaying-phase predictions

Seasonal growth rates of initial errors

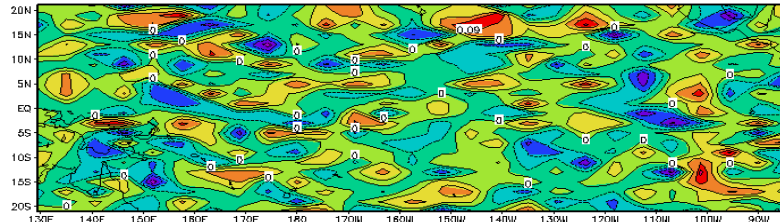


Prediction errors caused by CNOP and LSV

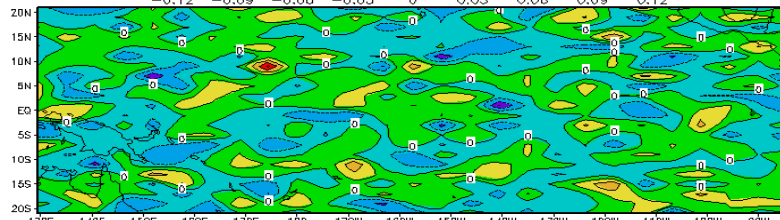
Nonlinearity increases the uncertainties of the predictions through spring

# Examples of random initial errors

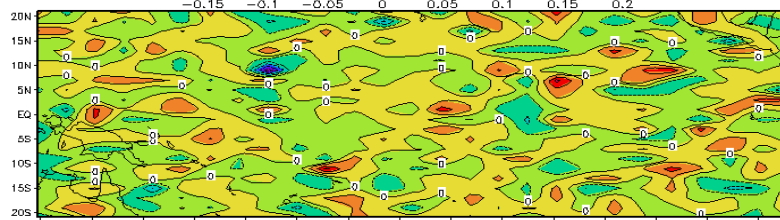
SSTA component ( $^{\circ}C$ )



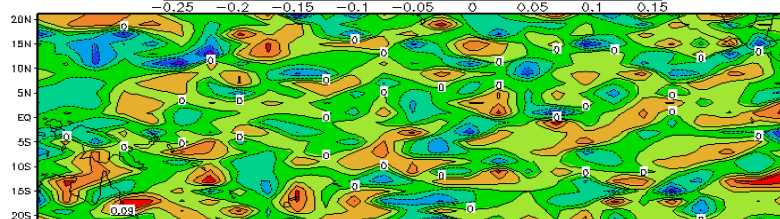
start month  
July



start month  
October

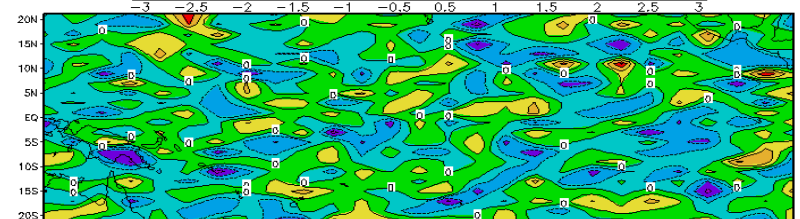
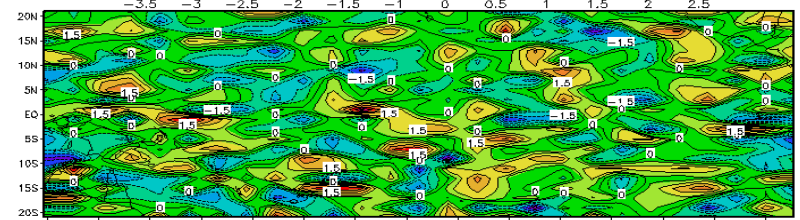
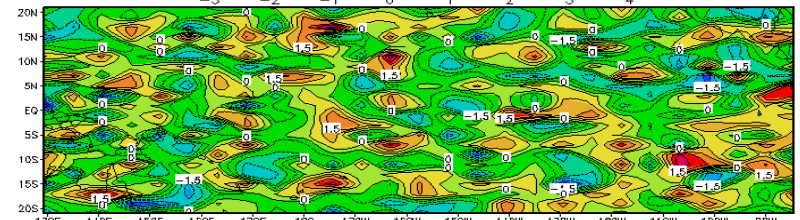
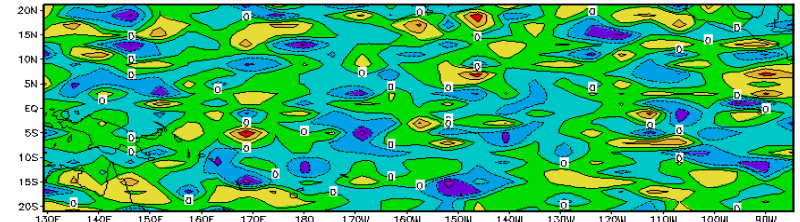


start month  
January



start month  
April

Thermocline depth anomaly component (m)



One case. Other cases have similar results

Small prediction errors  
of Nino-3 SSTA

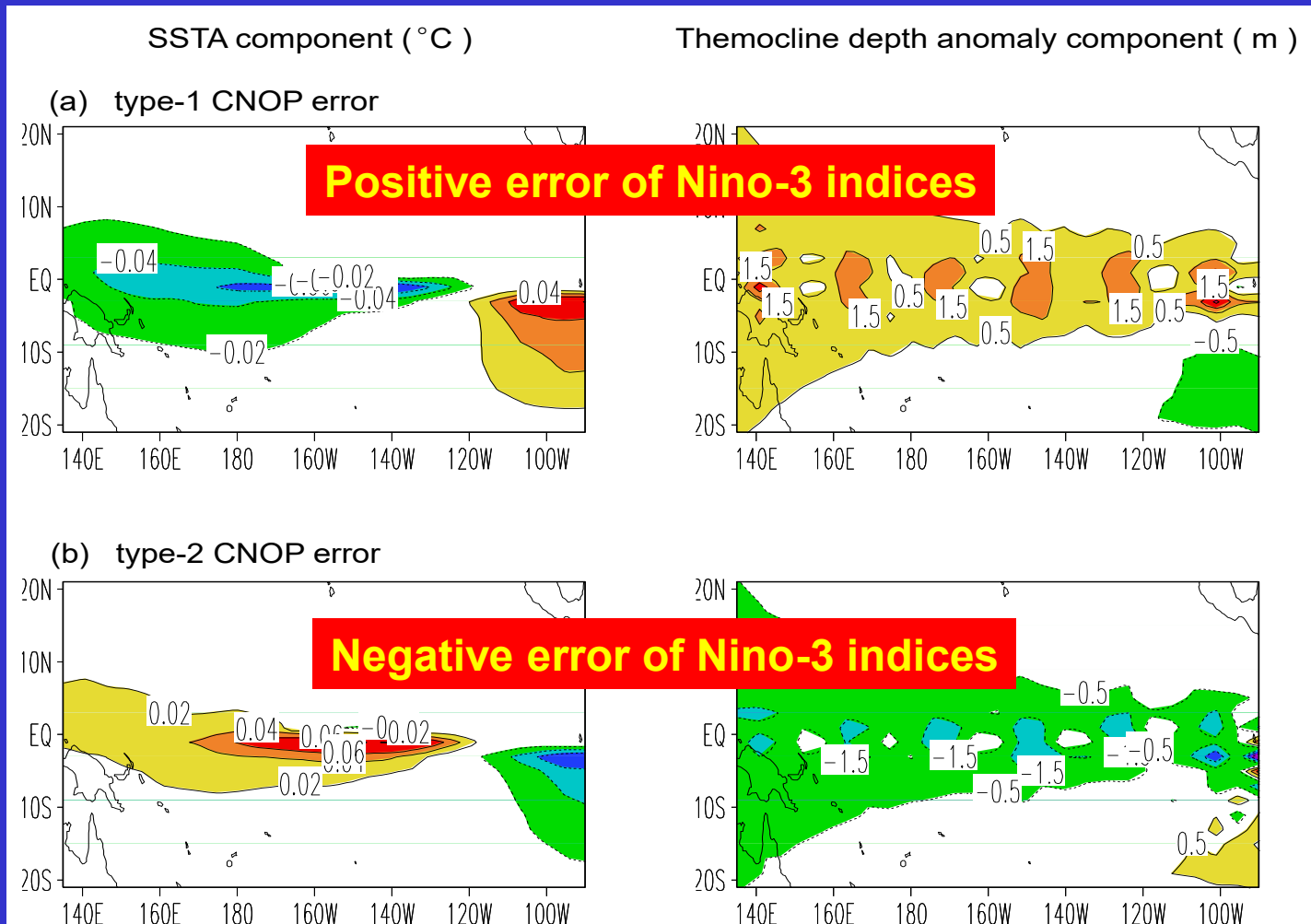
Start month: July in year (-1)

El Nino	JAS	OND	JFM	AMJ	E-Nino3
WR <sup>1</sup> <sub>Jan</sub>	-0.211	0.038	0.065	0.068	0.069
SR <sup>1</sup> <sub>Jan</sub>	-0.249	-0.077	0.077	0.299	-0.099
WR <sup>1</sup> <sub>Apr</sub>	-0.249	-0.034	0.002	0.052	0.034
SR <sup>1</sup> <sub>Apr</sub>	-0.216	0.044	0.112	0.196	0.105
WR <sup>1</sup> <sub>Jul</sub>	-0.216	-0.012	0.036	0.187	-0.083
SR <sup>1</sup> <sub>Jul</sub>	-0.257	0.001	-0.003	0.089	-0.055
WR <sup>1</sup> <sub>Oct</sub>	-0.210	0.057	-0.058	-0.022	-0.016
SR <sup>1</sup> <sub>Oct</sub>	-0.273	-0.046	-0.038	-0.012	-0.002

Random initial errors do not cause the SPB.

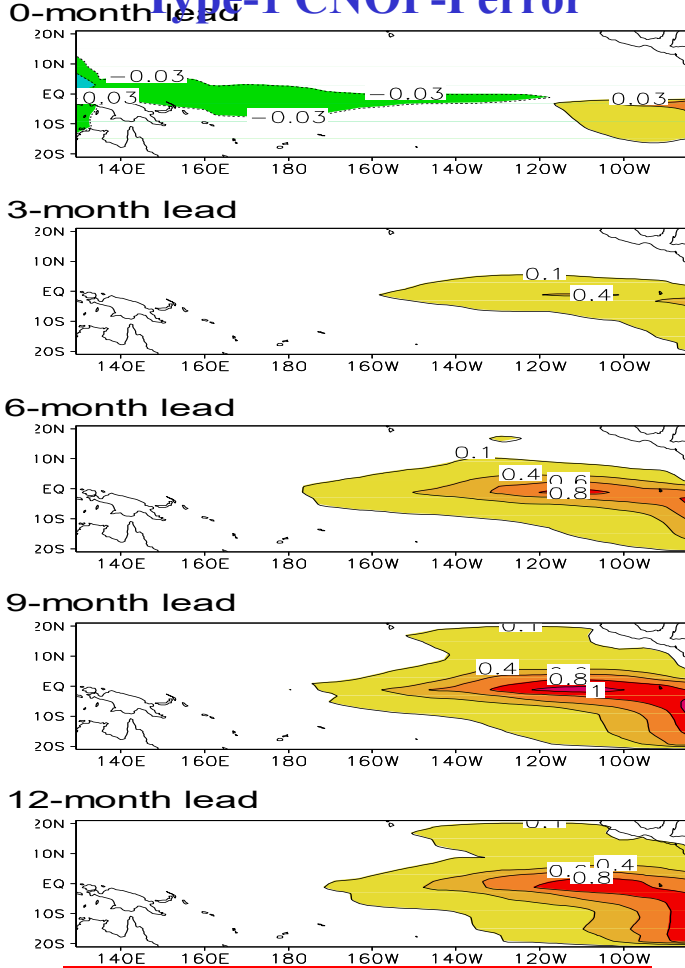
# 5. Spatial characteristic of the initial errors that cause a significant SPB

Cluster analysis method. Similarity coefficient (128 CNOP-I errors):



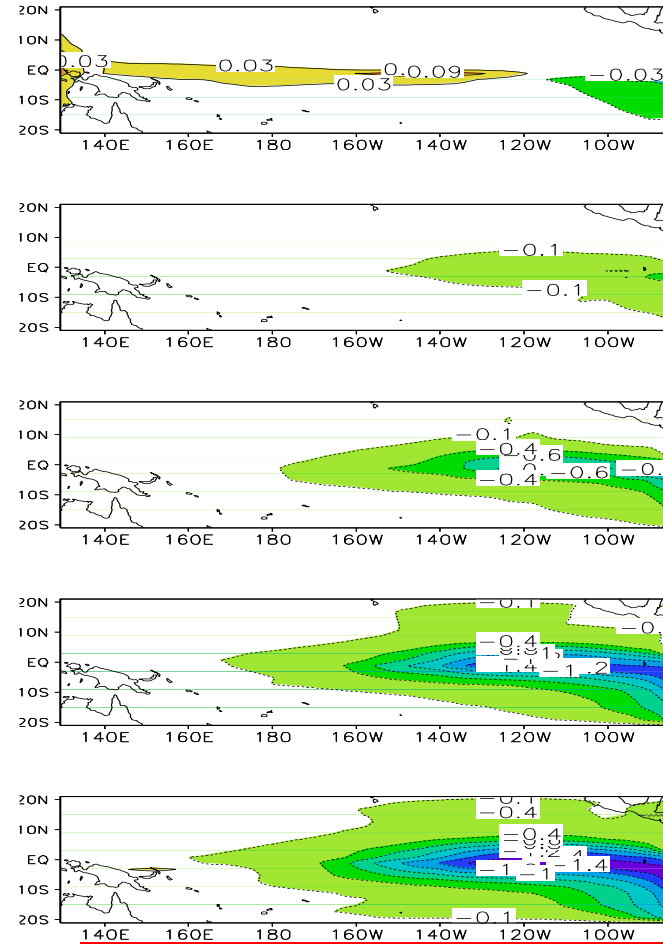
# Evolutions of two types of CNOP-I errors

(a) **Type-1 CNOP-I error**



**Positive error of Nino-3 indices**

(b) **Type-2 CNOP-I error**



**Negative error of Nino-3 indices**

**CNOP-type errors:  
a significant SPB**

**LSV-type errors:  
less significant SPB**

**Random initial errors  
and parameter errors:  
fail to cause a SPB**

```
graph TD; A["CNOP-type errors:  
a significant SPB"] --> D["A significant SPB: particular pattern of initial error"]; B["LSV-type errors:  
less significant SPB"] --> D; C["Random initial errors  
and parameter errors:  
fail to cause a SPB"] --> D;
```

**A significant SPB: particular pattern of initial error**

# 3 Decadal Variabilities of THC

THC is an important component of the climate system.

The decadal and interdecadal variabilities of THC in the Atlantic is thought to be responsible for AMO. So it becomes a hot topic.

The understanding of the mechanisms of variabilities is far from mature due to lack of the observations and theoretical researches.

- 1) rare observations on ocean;
- 2) low signal-noise ratio.

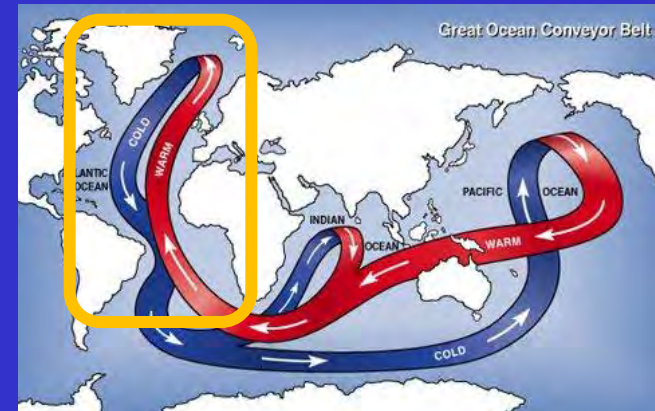
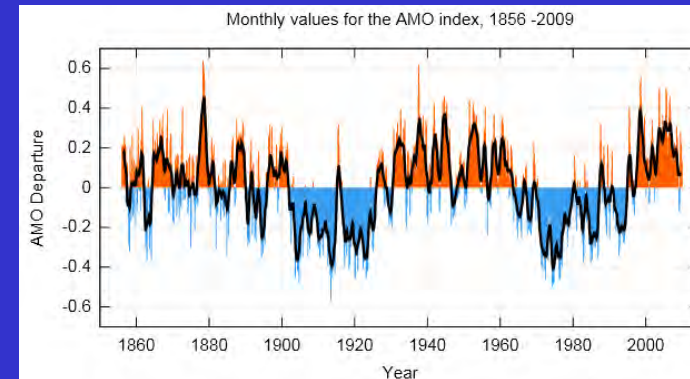


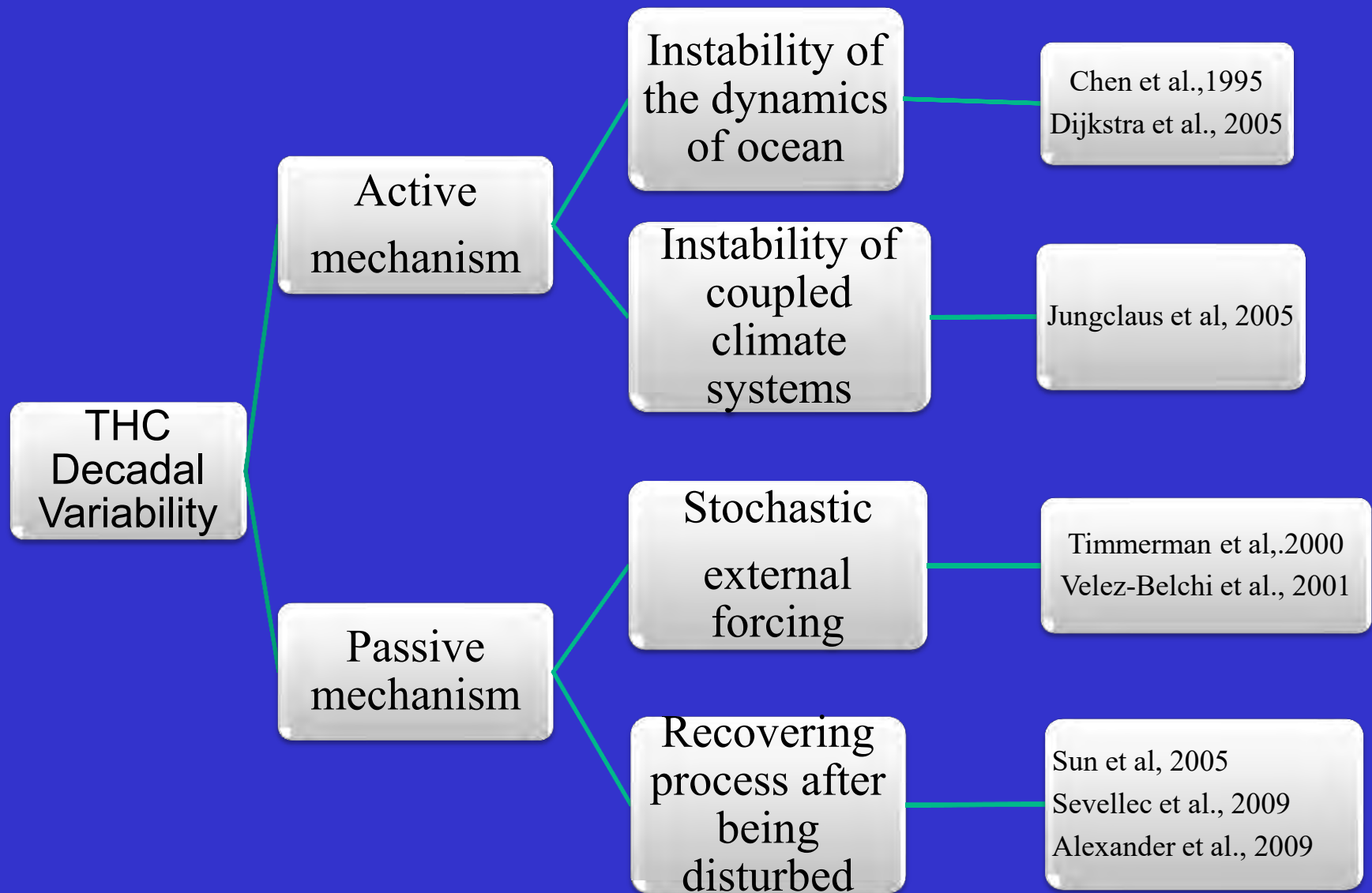
Image courtesy Argonne National Laboratory.



Data from

<http://www.cdc.noaa.gov/Correlation/amon.us.long.data>

# The existed mechanisms



# The Coupled Atmosphere-Ocean Model

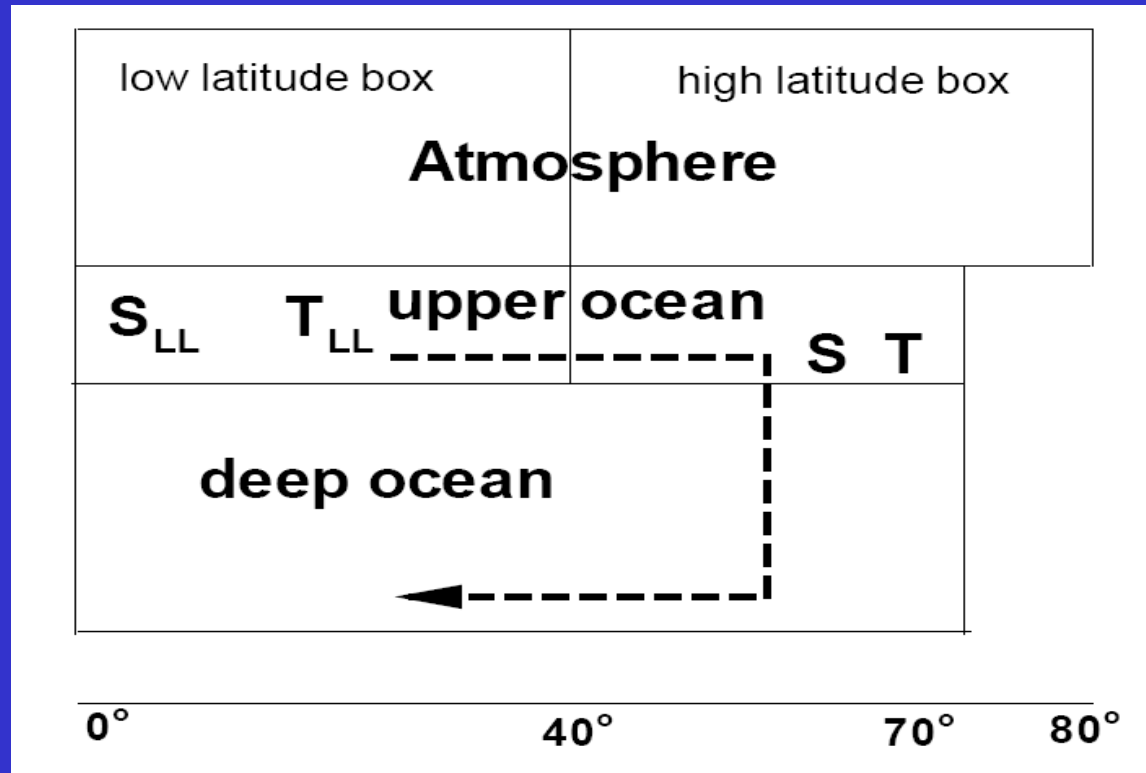


Figure 1: The coupled atmosphere-ocean boxes model (after Lohmann, et al., 1996)

# The Model Equation

The evolution of the perturbation :

$$\frac{dx}{dt} = Ax - \langle b, x \rangle x \quad (1)$$

$x = (T', S')$  represents the perturbations on the basic state of temperature and salinity.

$\langle \square, \square \rangle$  is inner product of two vectors.

$A$  is the parameter matrix.

Where  $\Psi' = \langle \mathbf{b}, \mathbf{x} \rangle = -c(\alpha T' - \beta S')$

is dimensionless flow rate.

If there is more fresh water entering the North Atlantic Ocean, the perturbation has  $S' < 0$  and  $\Psi' < 0$ , which is called *fresh perturbation*.

If there is less fresh water entering the North Atlantic Ocean, the perturbation has  $S' > 0$  and  $\Psi' > 0$ , which is called *salinity perturbation*.

# Decadal variation of THC

- The passive variabilities of THC is investigated by superposing initial perturbations to the thermohaline circulation.
- Firstly we choose a positive number  $\epsilon$  to measure the recovery of a perturbation.
- We use CNOPs to define recovering time  $t_{\delta}^{\epsilon}$ , which is the time period the CNOP with initial constraint condition  $\delta$  takes to recover to  $\epsilon$ .

# Decadal variation of THC

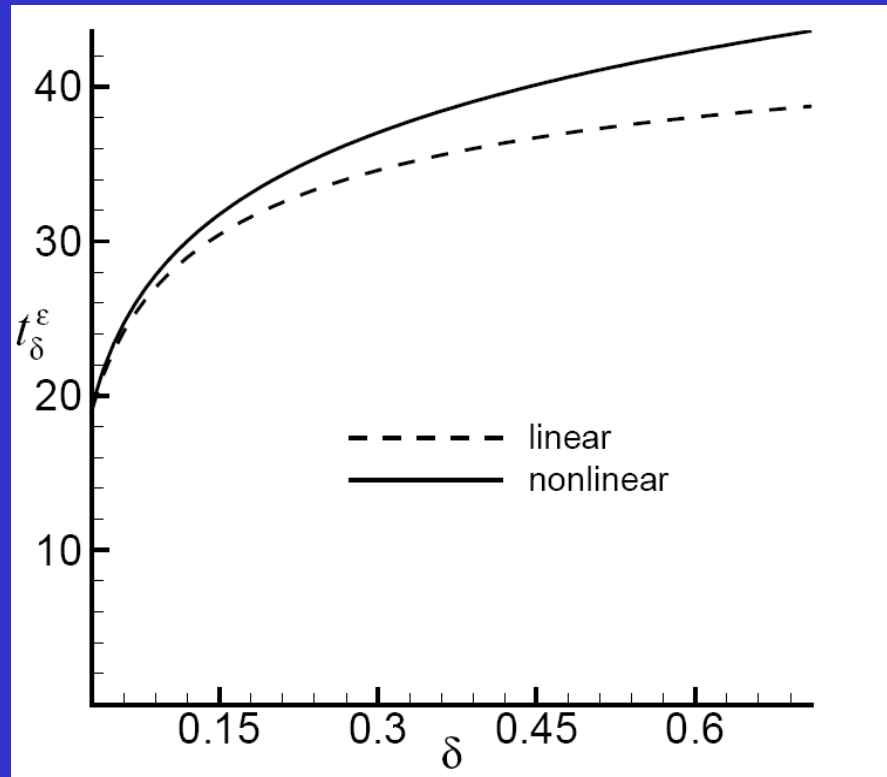


Figure 5: The recovering time  $t_{\delta}^{\epsilon}$  vs magnitude  $\delta$  of initial perturbation for  $\epsilon = 0.01$ . Dashed: linear results, solid: nonlinear results .

# Decadal variation of THC

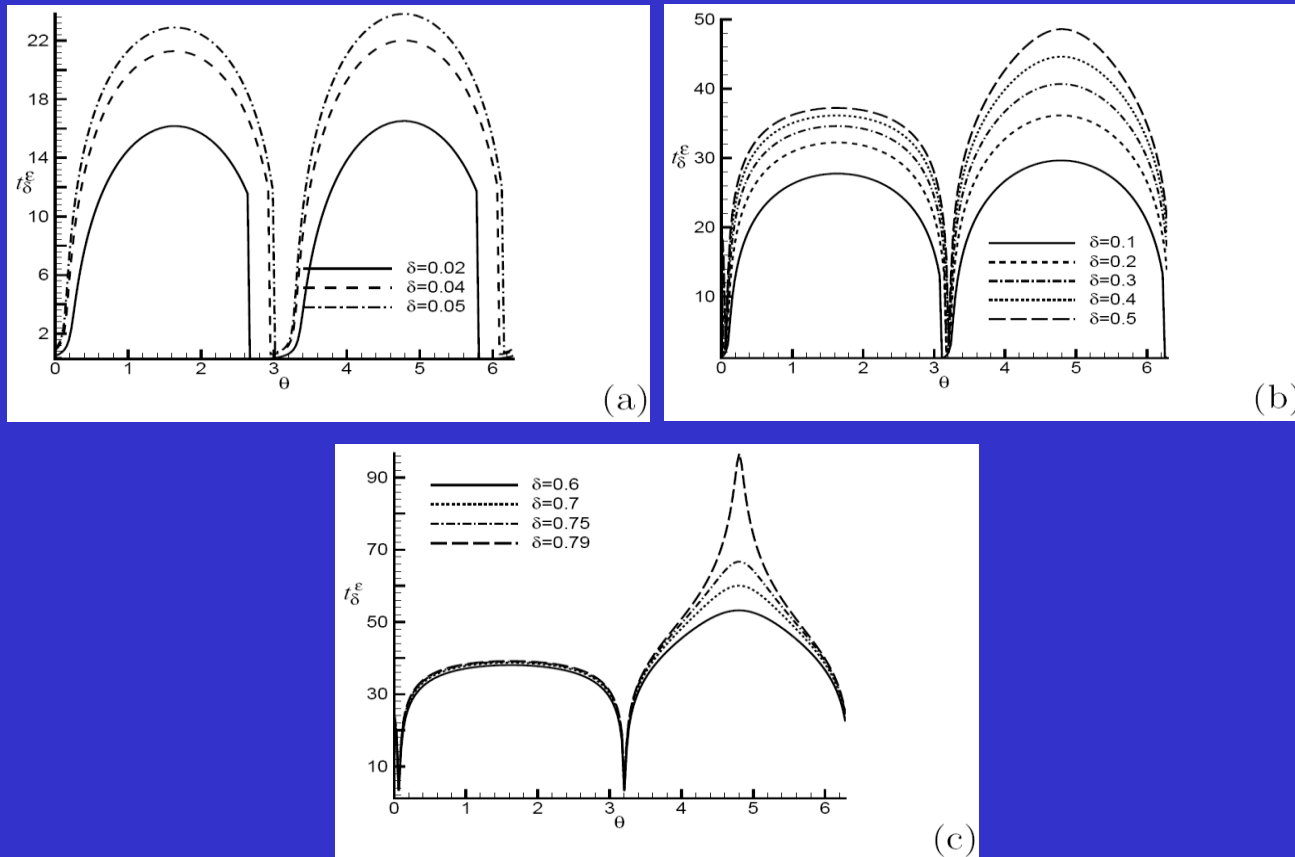


Figure 8: The plot of recovering time  $t_{\delta}^e$  vs. initial azimuth angle  $\theta$ . The initial magnitude of perturbations vary (a) from  $\delta = 0.02$  to  $\delta = 0.05$ , (b) from  $\delta = 0.1$  to  $\delta = 0.5$ , (c) from  $\delta = 0.6$  to  $\delta = 0.79$ .

# Decadal variation of THC

## Salinity flux perturbation:

- $\delta > 0.6$ , recovering time 40 years
- The recovery time saturation

## Fresh water perturbation :

- $\delta = 0.6$ , recovering time 53 years
- $\delta = 0.7$ , recovering time 67 years
- $\delta = 0.79$ , recovering time 96 years
- $\delta = 0.791$ , the breaking down of present THC.

# The mechanism of saturation and asymmetric evolution

## *Nonlinear feedback*

- **If there is no nonlinear effect , there is no saturation phenomenon.**
- **The evolution of initial perturbation will be symmetric one.**

# Summary of THC by box model

- *CNOP* leads to transient growth of THC and can causes decadal variations of THC.
- *CNOP* distinguish fresh water perturbation from salinity ones .The former is more sensitive than the later.
- *Nonlinear feedback* : an explanation to the sensitivity of fresh water perturbation and to the saturation of recovering time of salinity perturbation.

## 4.2 Results of OGCM:

### Model and its configuration

THCM: a 3D ocean general circulation model, which is a fully implicit model and can produce the tangent linear and adjoint matrix.

Domain: [286W, 350W] \* [10N, 74N]; without geometry.

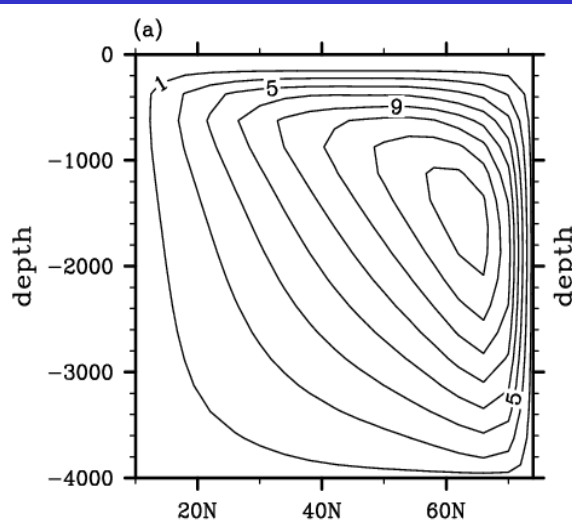
Resolution: 40\*40\*250m

Uniform basin depth: 4000m

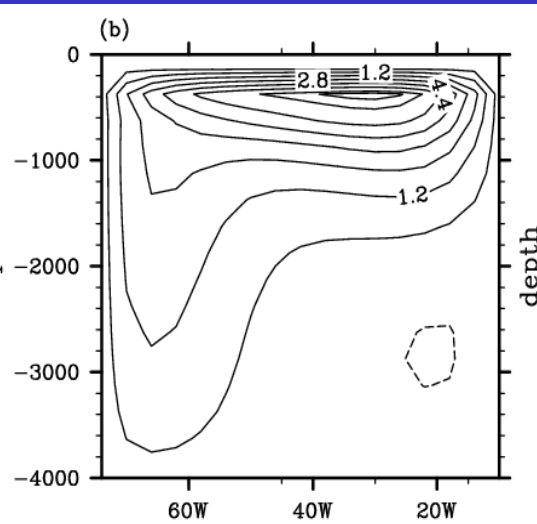
Time step: from 0.7-14 days

# Steady/basic state

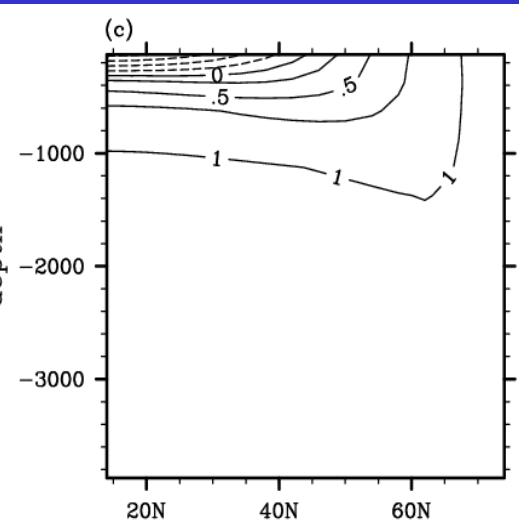
MOC (Sv)



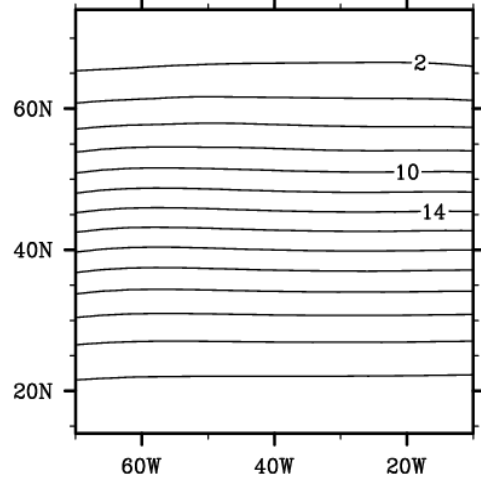
ZOC (Sv)



Zonal mean density ( $\text{kg/m}^3$ )

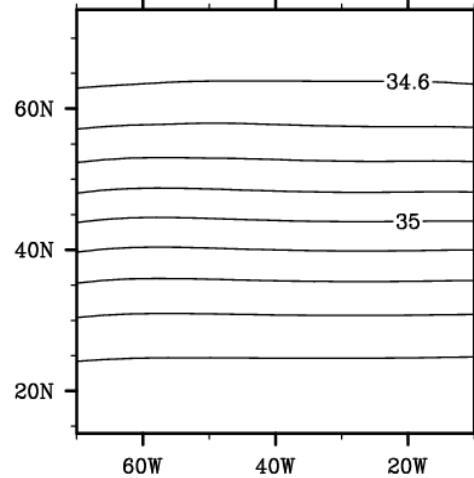


(d)



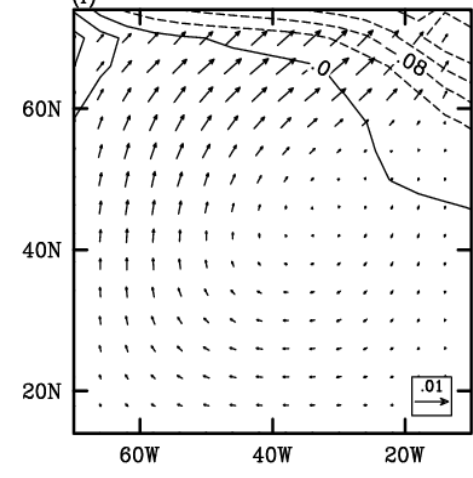
SST(°C)

(e)



SSS(psu)

(f)



Upper layer velocities averaged over the upper 1500 m (m/s)

# Optimization configuration

Cost function:

$$J = \int_{\text{South}}^{\text{North}} \left[ \int_{\text{West}}^{\text{East top}} \int_L V' \cos \psi d\theta dz \right]^2 d\psi$$

$\psi$ : latitude  
 $\theta$ : longitude

(Alexander and Monahan 2009)

$v'$ : meridional velocity anomaly.

North, South, East, West, Top : boundaries.

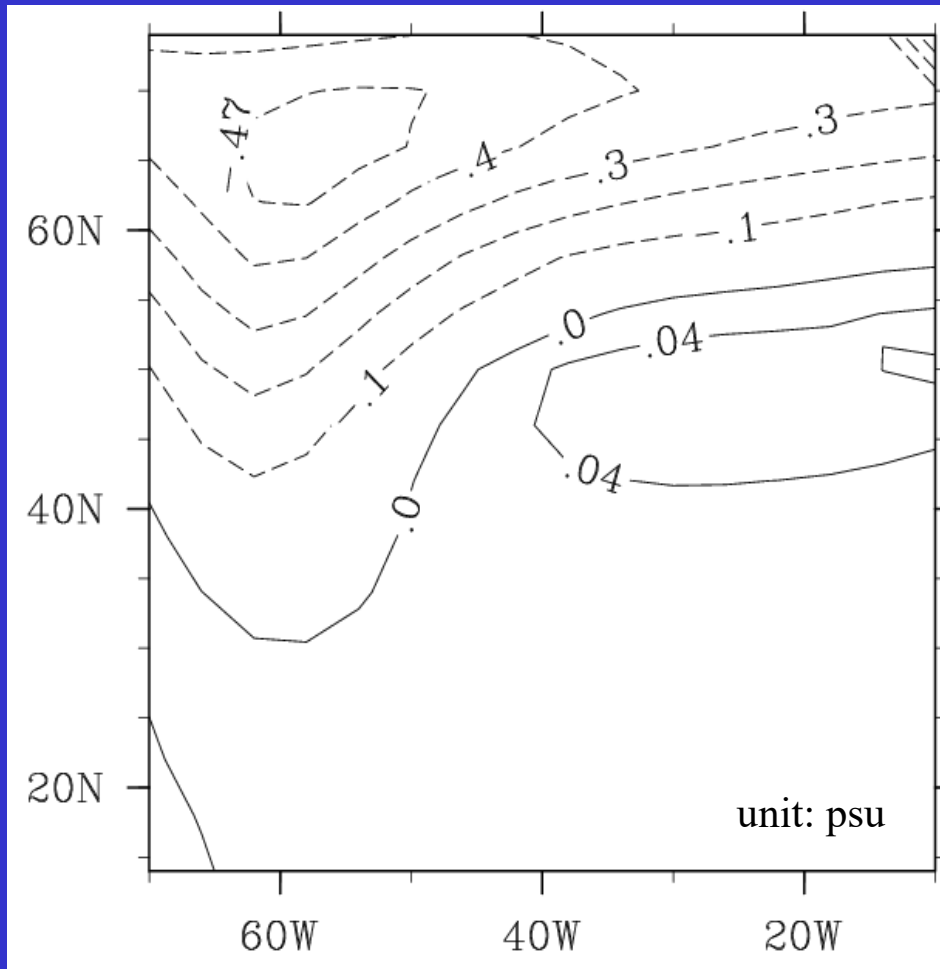
$L$  : the depth of streamfunction maximum,  $L=-1500\text{m}$

The constraints of initial perturbations:  $\sqrt{\sum SSS'^2} \leq 3.2$

Optimal time: 10yr

By these configuration, we want to seek a kind of perturbations, which could weaken THC the most for a delay of 10yr.

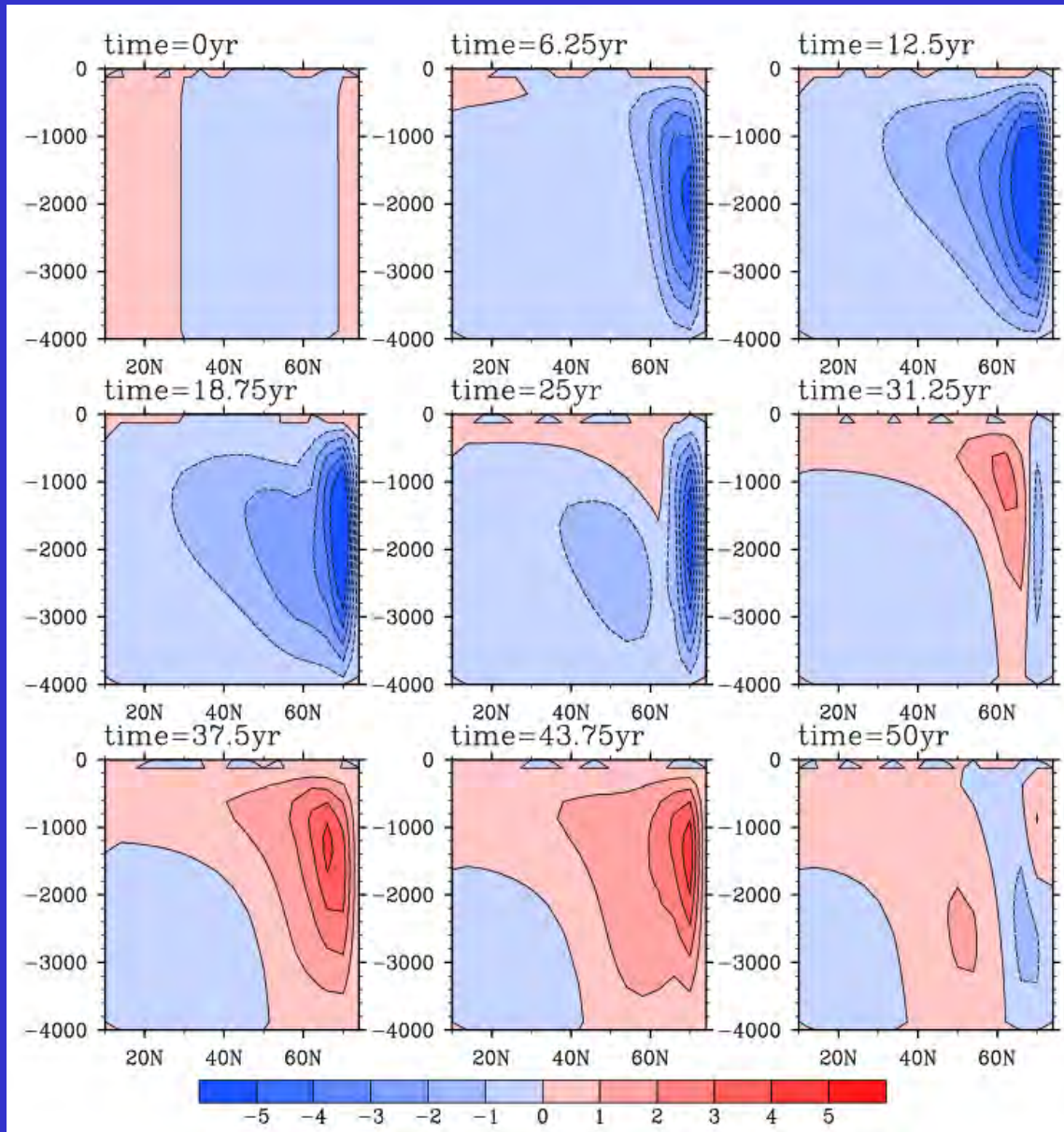
# Optimal initial SSS perturbations



Minimum: -0.48 psu,  
corresponding to the amplitude of  
GSA (Great Salinity Anomaly)  
events.

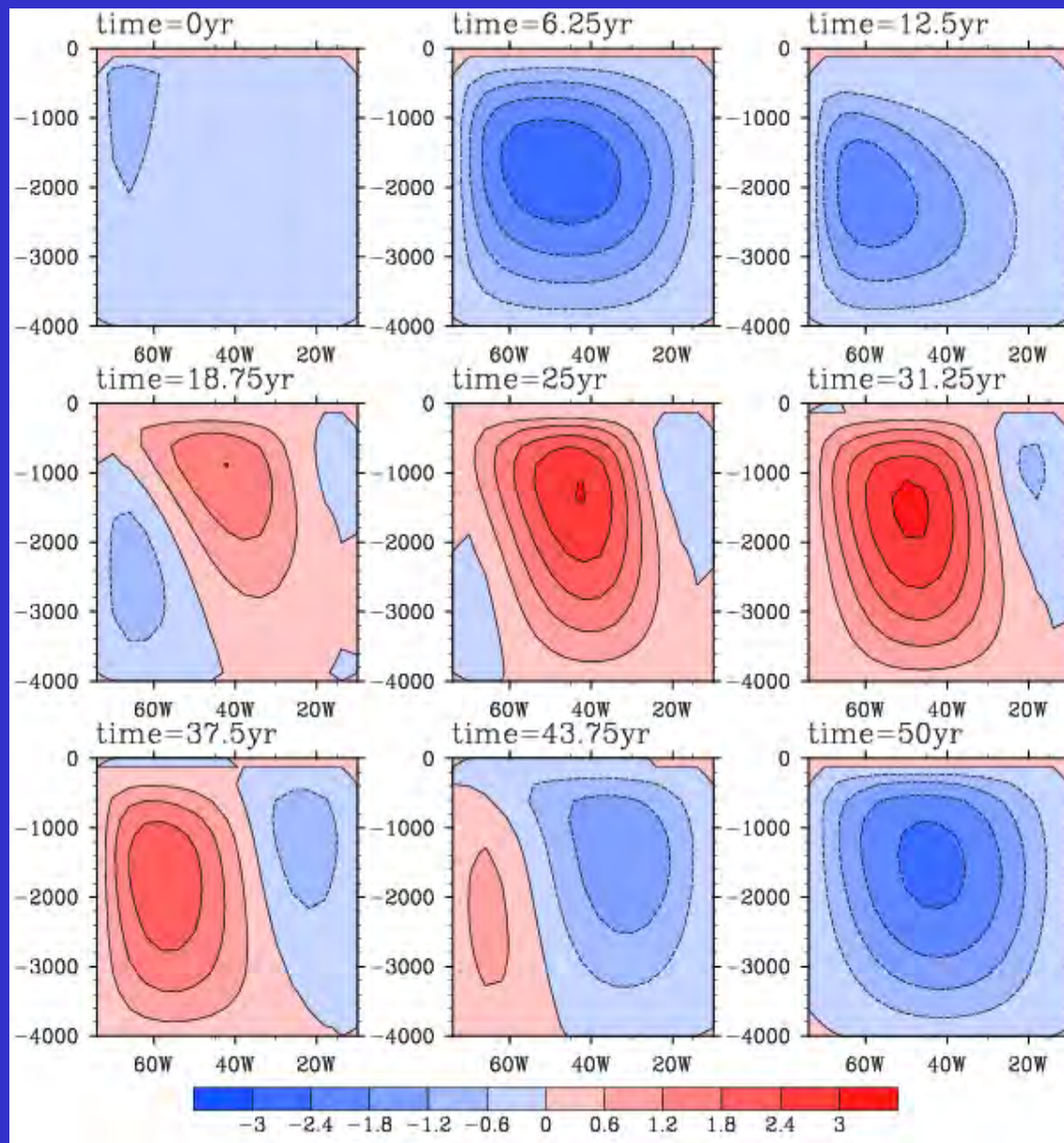
Strong meridional gradient and  
weak zonal gradient.

# Time slices of MOC anomaly the perturbation induced



The MOC decreased and then increased. The period is 50 yr.

# Time slices of ZOC anomaly the perturbation induced

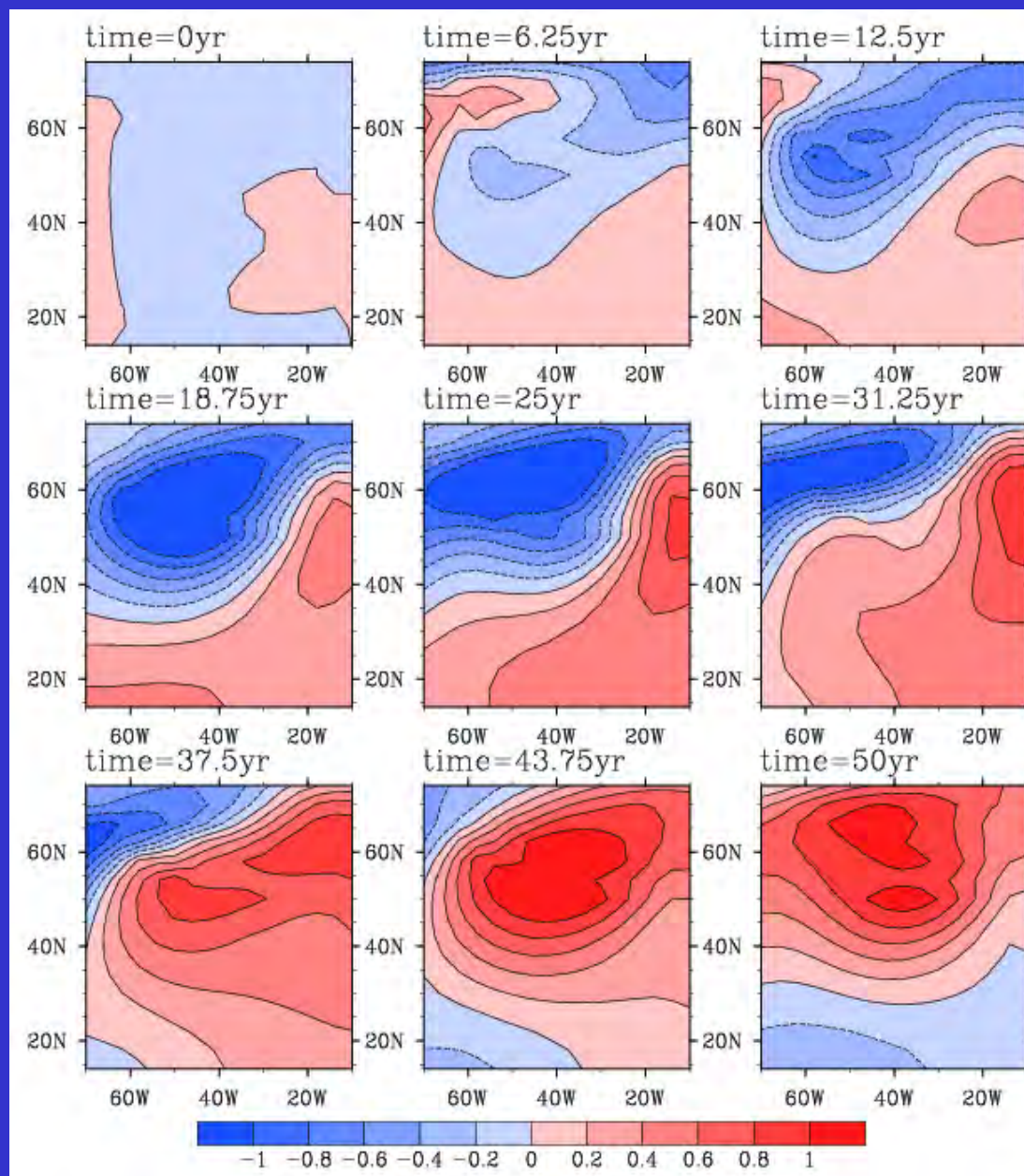


The ZOC decreased, increased and then decreased.

The period is also 50 yr.

The phase leads that of MOC.

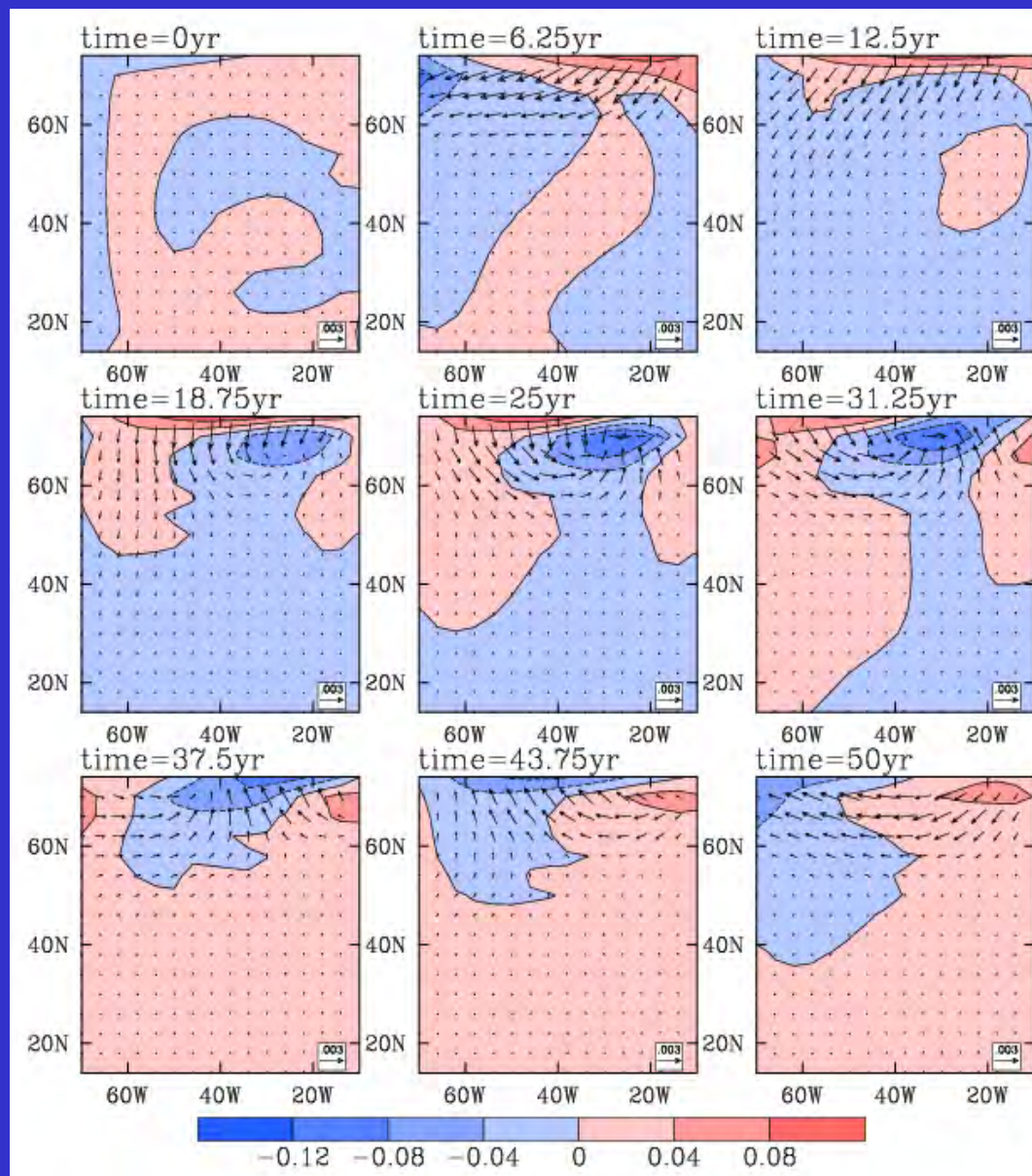
# Time slices of SSTA the perturbation induced



The variations of SSTA show a signal of AMO

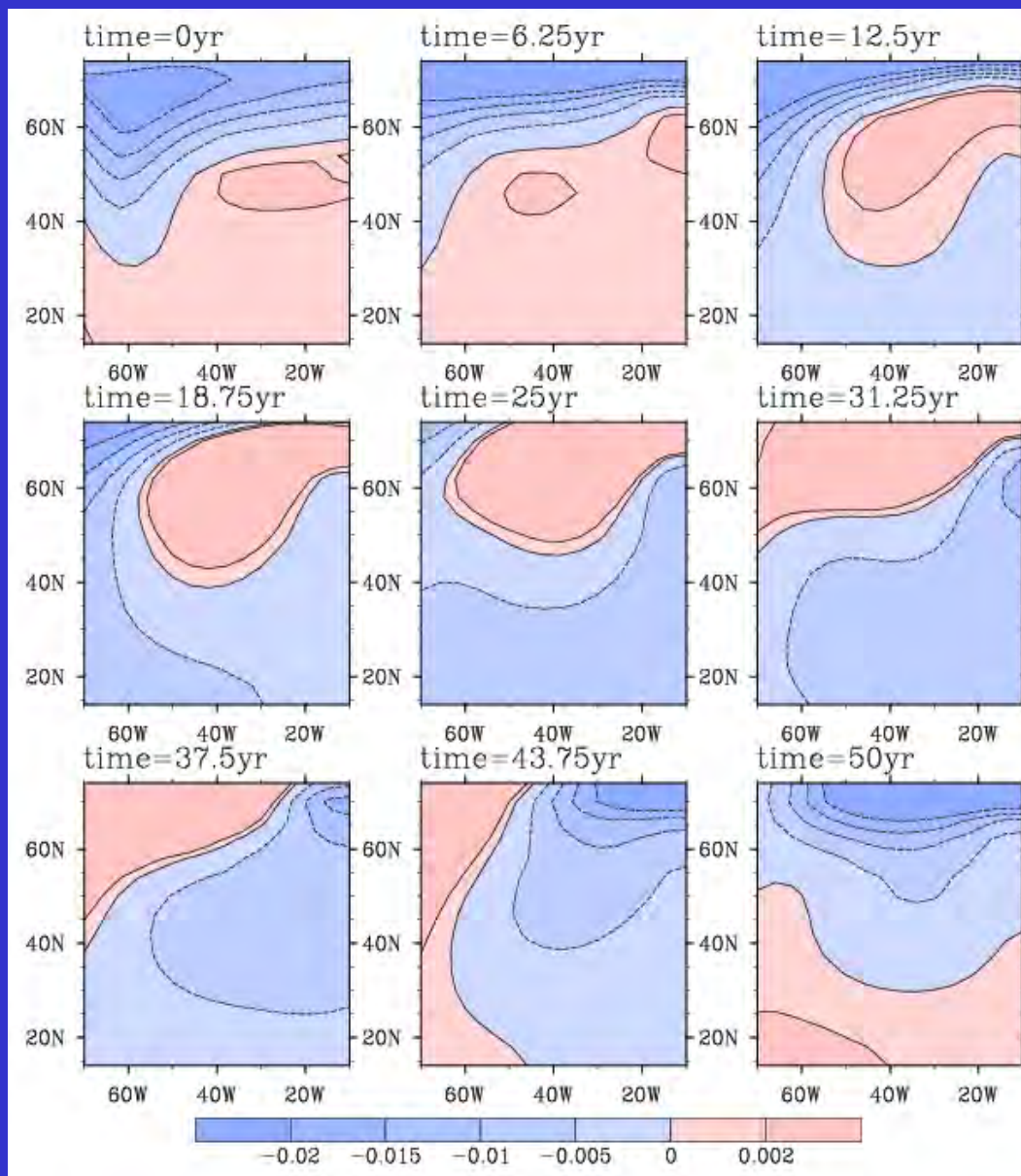
- 1 Basin-scale warming and cooling.
- 2 The period is 50yr.
- 3 Westward propagating of SSTA anomaly

# Time slices of surface velocities anomaly



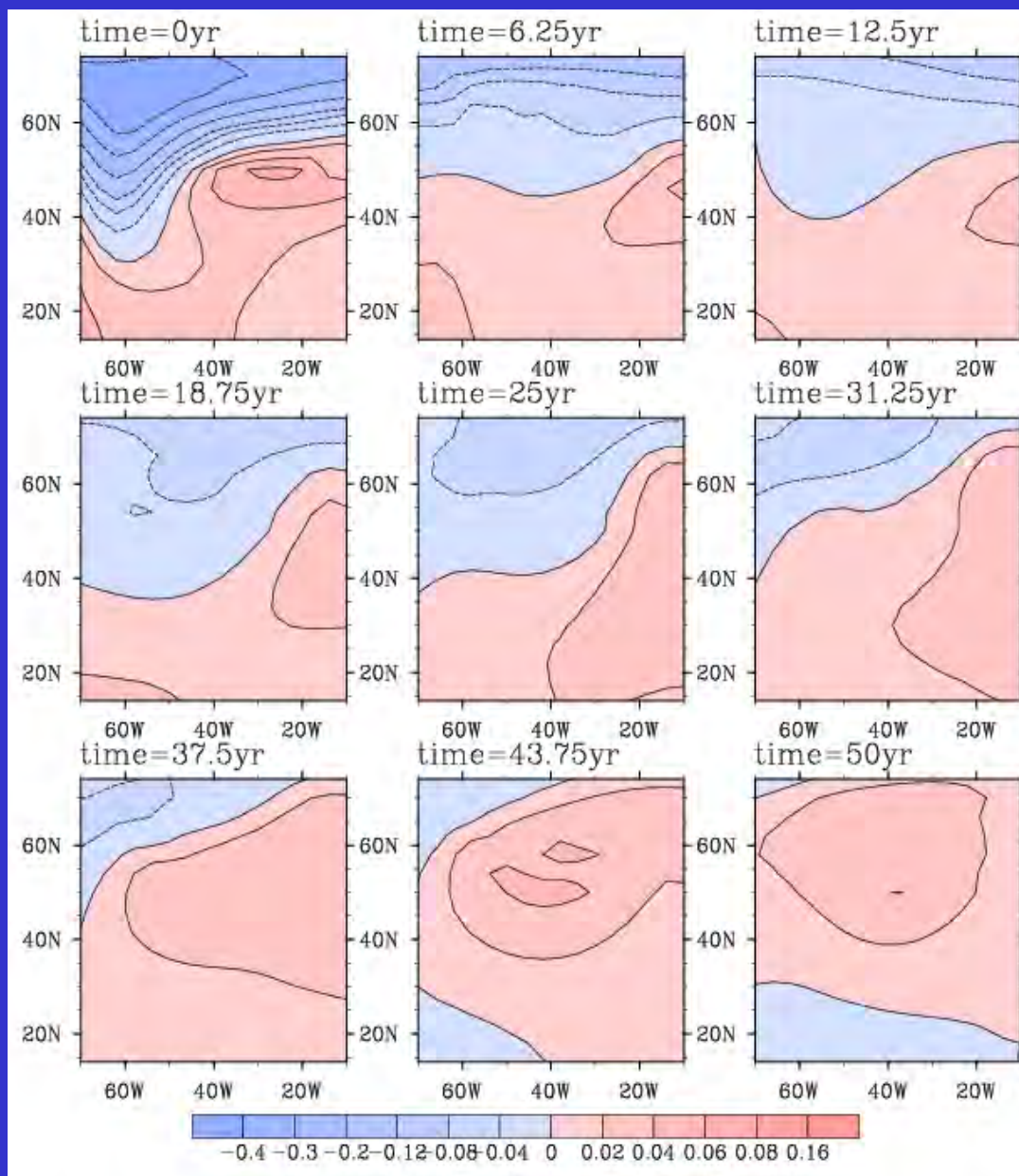
Westward propagating  
of velocities anomaly

# Time slices of vertical mean density anomaly



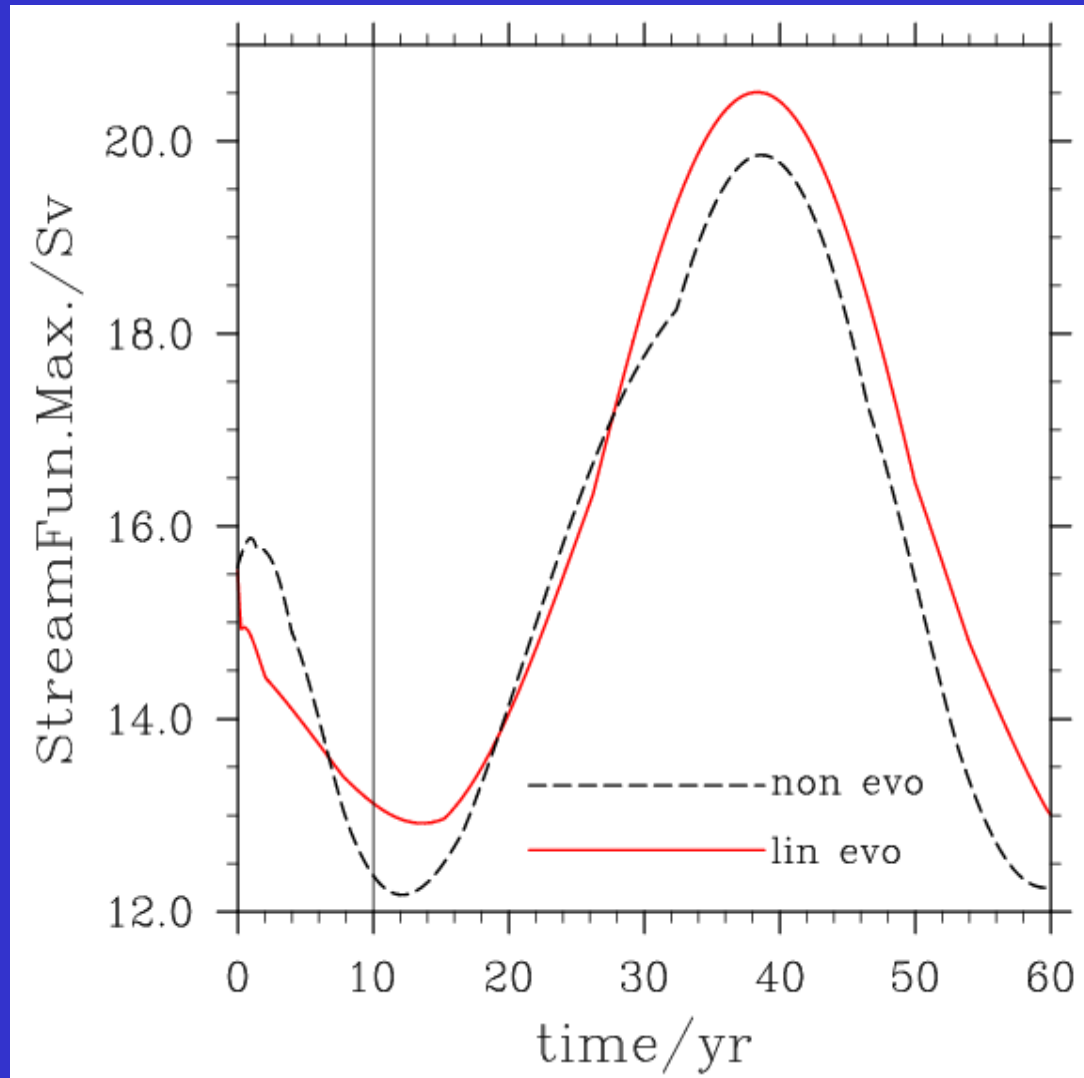
Westward propagating  
of density anomaly

# Time slices of SSS anomaly



Westward propagating  
of SSS anomaly

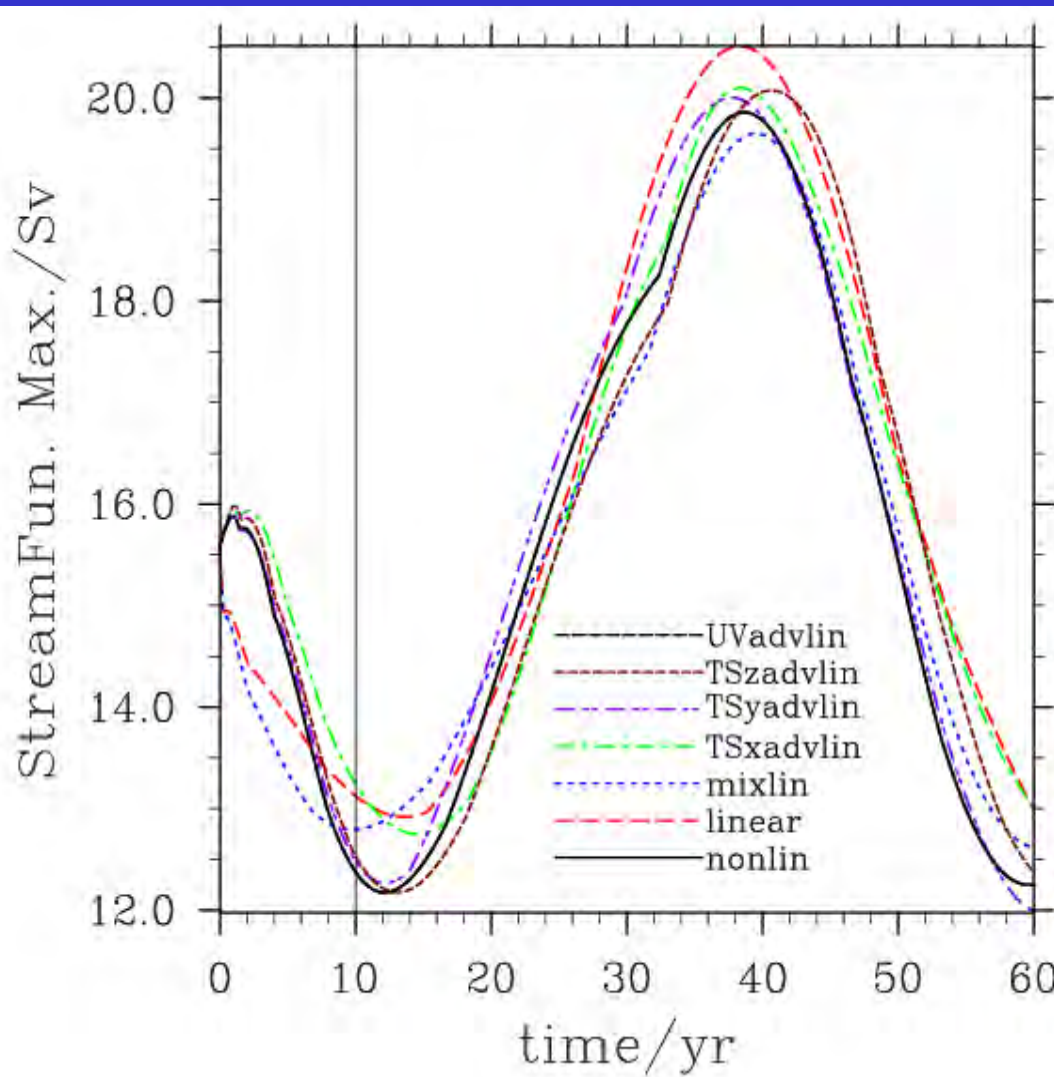
# Variations induced by initial perturbations



- 1 THC is weakened by 4 Sv(25% of the intensity of steady state)
- 2 These perturbations have induced decadal variations, with period of 50yr.
- 3 The nonlinear terms is important.

# Variations induced by initial perturbations after some nonlinear terms are linearized

To isolate the influence of each nonlinear term on the intensity of THC, we have linearized each nonlinear term, respectively.



- 1 From 0 to 4yr, the nonlinear term of parameterization of convection (mix for simplicity) is important.
- 2 From 4 to 8yr, the nonlinear terms of zonal density advection and mix are important.
- 3 From 8 to 15yr, the nonlinear terms of zonal density advection and mix are still important.
- 4 The nonlinear terms in momentum equations are not important.

# Summary of THC by OGCM

- 1 The initial perturbations of SSS can induce the decadal variabilities of THC.  
  
And cause an amplitude of the variations of 4 Sv ( 25% of the basic state) with the period of 50 yr.
- 2 The physics of oscillations involves the interaction of zonal density gradient anomaly, meridional density gradient anomaly, zoc and moc anomaly, according to the thermal wind relation.
- 3 The perturbations obtained by LSV are similar to those by CNOP, except a stronger westward extending of positive perturbations in the south of the region. Compared to the perturbations by LSV, those by CNOP can induce stronger decadal variations of THC, which indicate that CNOP approach is a more effective tool to investigate the cause of the decadal variabilities of THC.

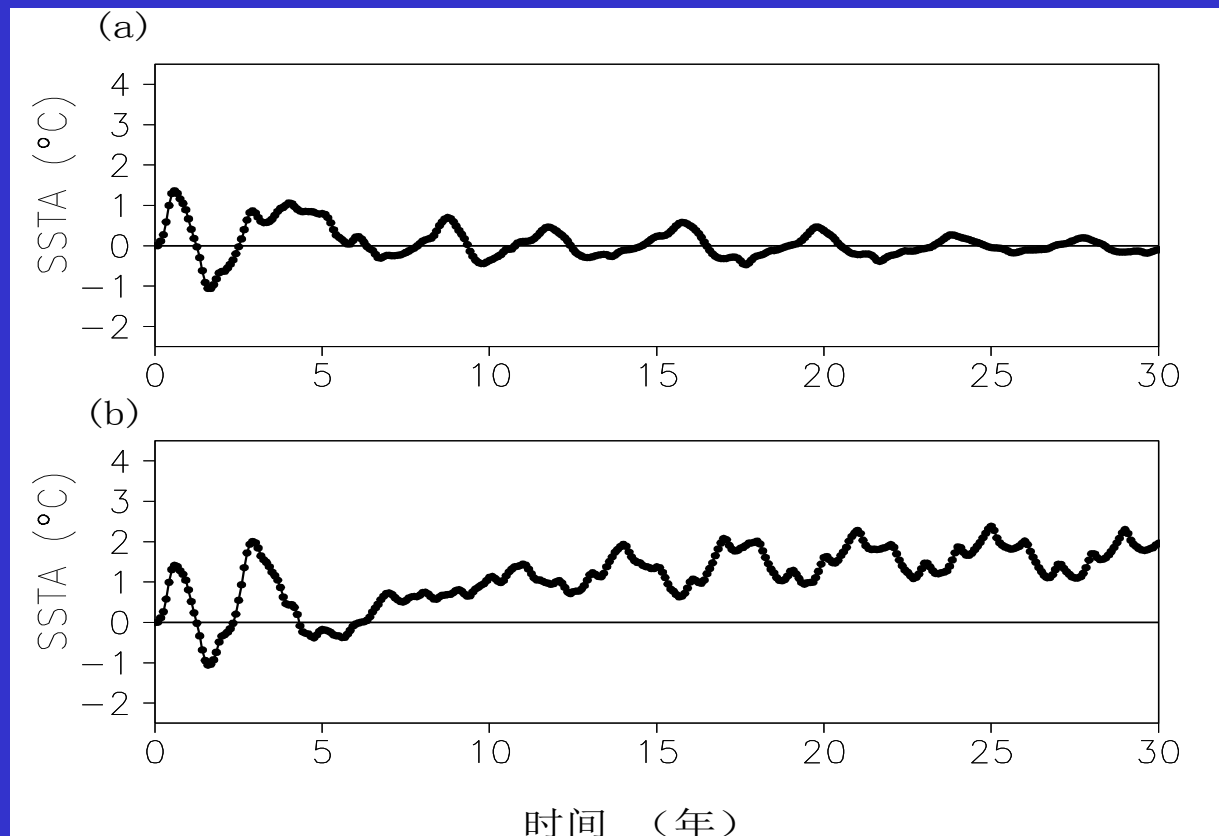
Thank you!



**Model dependent?**

**Localized region of CNOP-I errors: target observation;**

**In calculating CNOP-P, the constraint bounds are determined to make the model ENSO events maintaining the irregular oscillation similar to observed ENSO.**



## Constraint bound of nine parameters

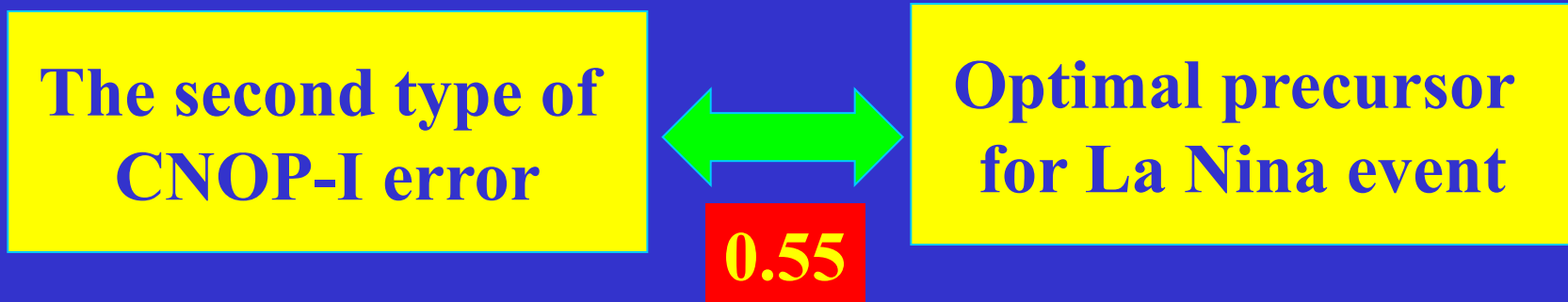
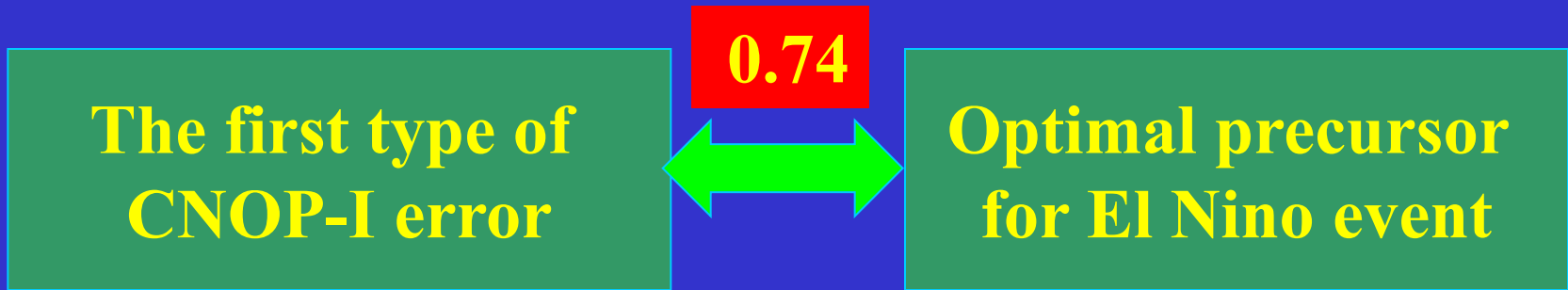
Parameter	Constraint Bound	Parameter	Constraint Bound	Parameter	Constraint Bound
$\alpha$	0.1%	$\eta$	0.02%	T2	3%
$\beta$	4%	T1	0.1%	b2	2%
$\varepsilon$	0.3%	b1	1%	$\sigma$	1%

## E.4 Seasonal growth rate of prediction errors caused by random error on model parameters

One case: Start month July in year(-1)

El Nino	JAS	OND	JFM	AMJ	$E_{Ni\tilde{n}o-3}$
WR <sub>1</sub>	0.012	0.013	0.020	0.034	0.014
WR <sub>2</sub>	0.034	0.469	0.754	0.444	0.164
WR <sub>3</sub>	0.067	0.009	0.000	0.049	0.016
WR <sub>4</sub>	0.032	0.002	-0.016	0.004	0.000
SR <sub>1</sub>	0.001	0.007	0.010	0.024	-0.007
SR <sub>2</sub>	0.005	0.004	0.007	0.014	-0.004
SR <sub>3</sub>	0.005	0.002	0.004	0.004	-0.002
SR <sub>4</sub>	0.044	0.037	-0.010	-0.022	0.005

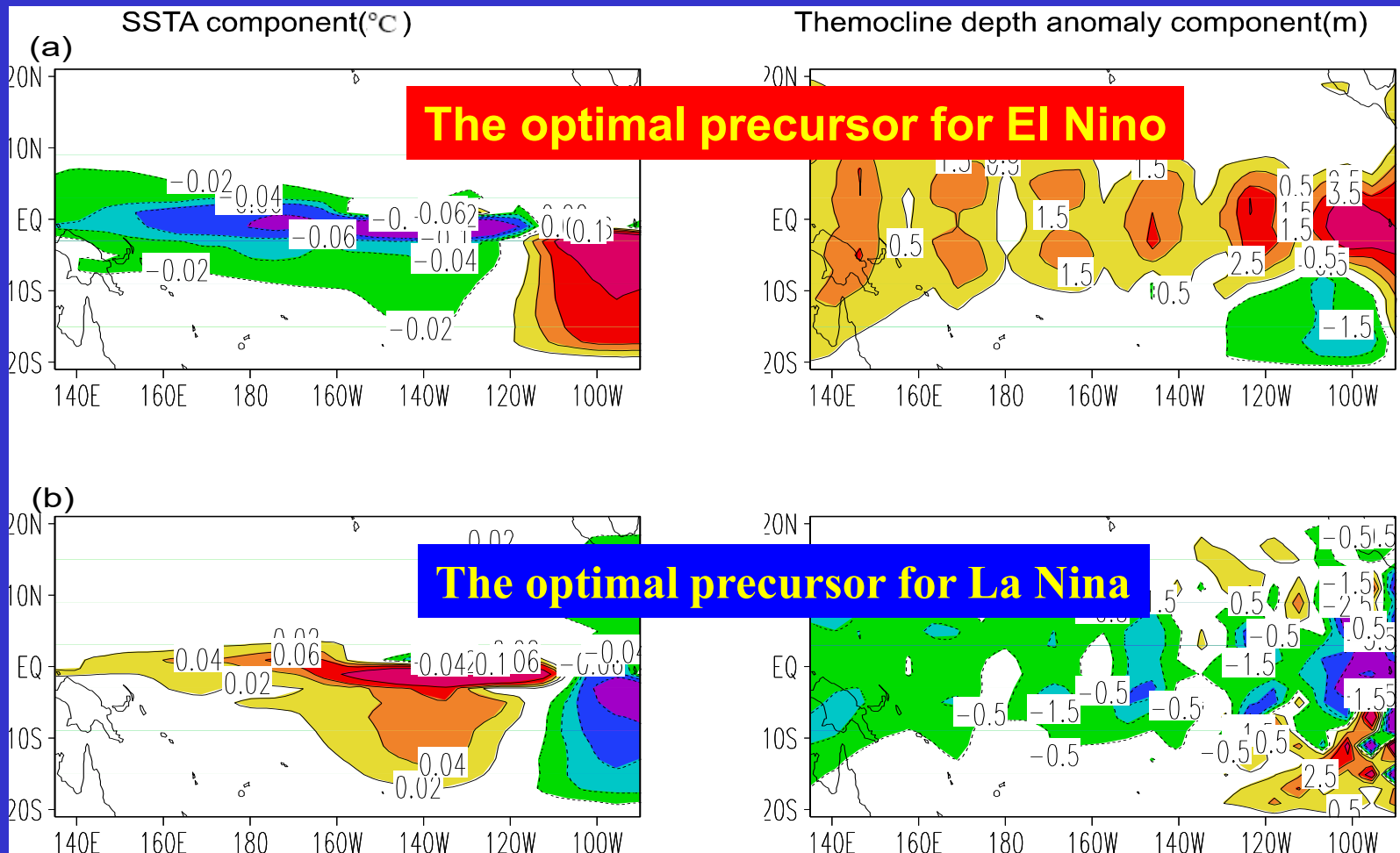
# Similarity coefficient



# The optimal precursors for El Nino and La Nina

(the initial anomalies that evolve into El Nino and La Nina events most probably)

## CNOP-I and local CNOP-I type initial anomalies



**E. Seasonal growth rates of  
prediction errors caused by  
model errors**

$$\text{CNOP-I} \longrightarrow \|\vec{u}_N(t)\| \longrightarrow \gamma(t)$$

One year is divided into four quarters.

Computing the slope  $\kappa$  of the curve  $\gamma(t)$  at different quarter.

$\kappa > 0$  ( $\kappa < 0$ )      Error increasing (decreasing)

$|\kappa| \uparrow$       Error increasing  
or decreasing  $\uparrow$

## E.1 Seasonal growth rates of prediction errors caused by CNOP-P error

Cost function related to CNOP-P in the ZC model

$$J(\bar{p}'_{cnop}) = \max_{a_i \leq p'_i \leq b_i} \|\bar{T}'(\tau)\|_2, \quad i = 1, \dots, n$$

$\tau$  : optimization time interval, 12 months

$\bar{T}'$  : prediction error of Nino-3 SSTA

$a_i \leq p'_i \leq b_i$  : constraint condition of model parameters

$\bar{p}'_{cnop}$  : CNOP-P

## The cost function related to the CNOP-I

$$J(\vec{u}_{0\delta}) = \max_{\|\vec{u}_0\|_2 \leq \delta} \|\vec{T}'(\tau)\|_2$$

$\tau$  : optimization time interval, 12 months

$\vec{T}'$  : prediction error of SSTA

$\vec{u}_0$  : non-dimensional initial error of SSTA and thermocline depth anomaly.

$\|\vec{u}_0\|_2 \leq \delta$  : constraint condition of initial errors

# **D. Perfect model predictability experiments**

## **D. Perfect model predictability experiments:**

investigating the characteristic of the initial errors that cause a significant SPB **along the thinking of hindcast experiments by performing perfect model predictability experiments**

CNOP pattern describes a characteristic of the initial errors that cause a significant SPB.

In realistic predictions, CNOP is not computed.

Whether or not there exist such initial errors in realistic predictions, at least in hindcast experiments?

## **D.1 Experiment strategy**

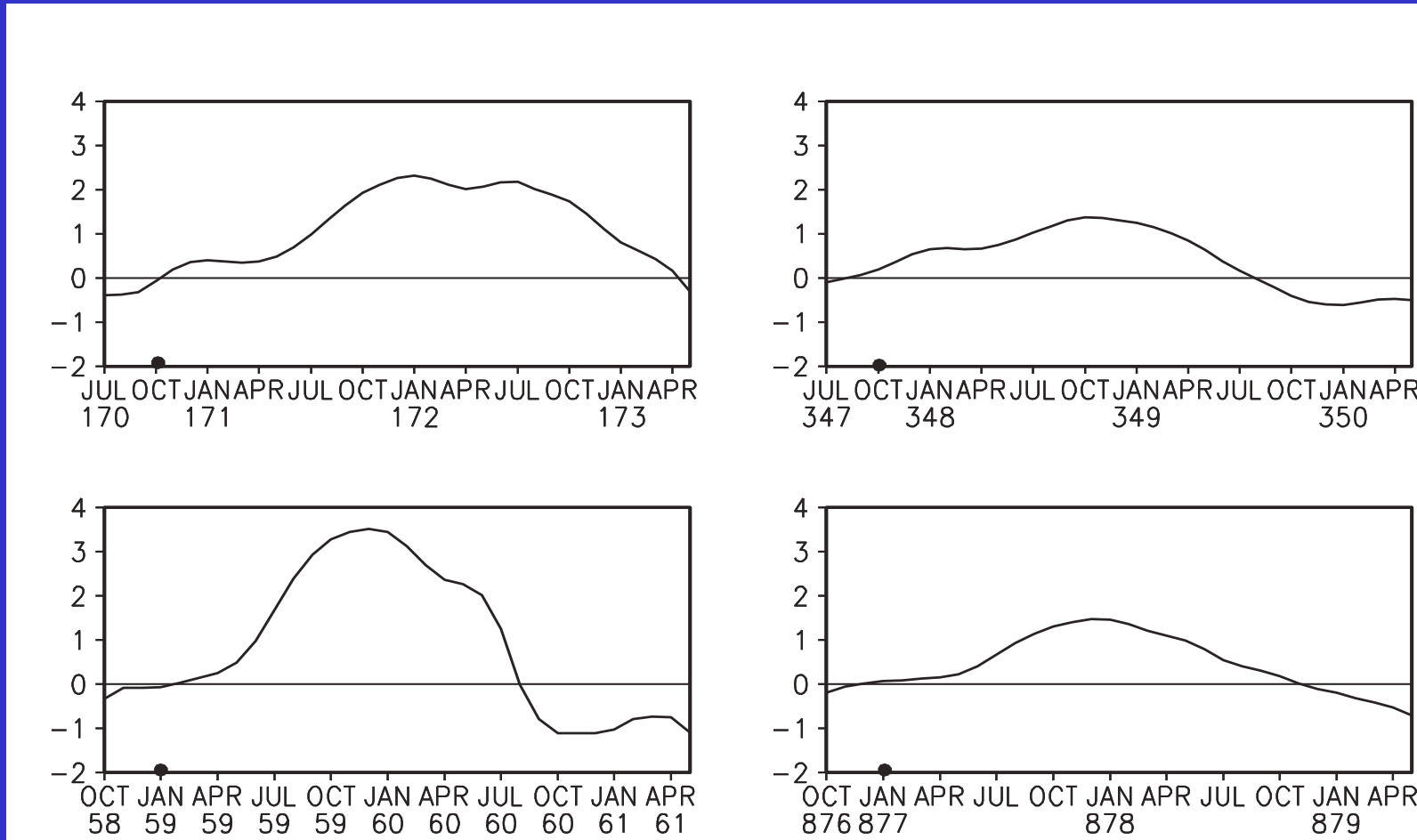
**Integrating ZC model for 1000 model years**

**Divide the 1000 years into ten time intervals  
(0-99, 100-199, ..., 900-999)**

**Choose two strong and two weak El Nino events  
A total of 40 El Nino events.**

**12 ones with initial warming time in Jan-Apr;  
28 ones in Sep-Nov.**

# Predicting these El Nino events with a leading time 12 months



Representatives of model El Nino events. **Left column:** Two strong El Nino events with initial warming time October and January; **Right column:** as in left column except for weak El Nino events.

Initial uncertainties: scaling the model **SSTA** and **thermocline depth anomaly** in each month of the 4 years preceding each El Nino year

48 initial error patterns, 48 predictions of each El Nino events.

## D.2 Seasonal growth rates of initial uncertainties

For the strong El Nino with initial warming time October

Table 1. Seasonal growth rates of Types-I and -II errors for  
the strong El Niño with initial warm in October

SSTA errors	OND	JFM	AMJ	JAS	$E_{Nino-3}$
Error - 11	0.312	1.695	<b>5.833</b>	4.657	-1.294
Error - 12	0.521	1.971	<b>5.819</b>	4.611	-1.322
Error - 13	0.622	1.848	<b>4.269</b>	<b>5.743</b>	-1.299
Error - 14	0.195	1.651	<b>6.170</b>	4.913	-1.334
Error - 21	0.093	0.977	<b>2.891</b>	1.517	0.561
Error - 22	0.114	1.116	<b>2.551</b>	1.363	0.528
Error - 23	0.183	1.146	<b>2.923</b>	1.647	0.594
Error - 24	-0.060	0.739	<b>3.173</b>	2.052	0.612

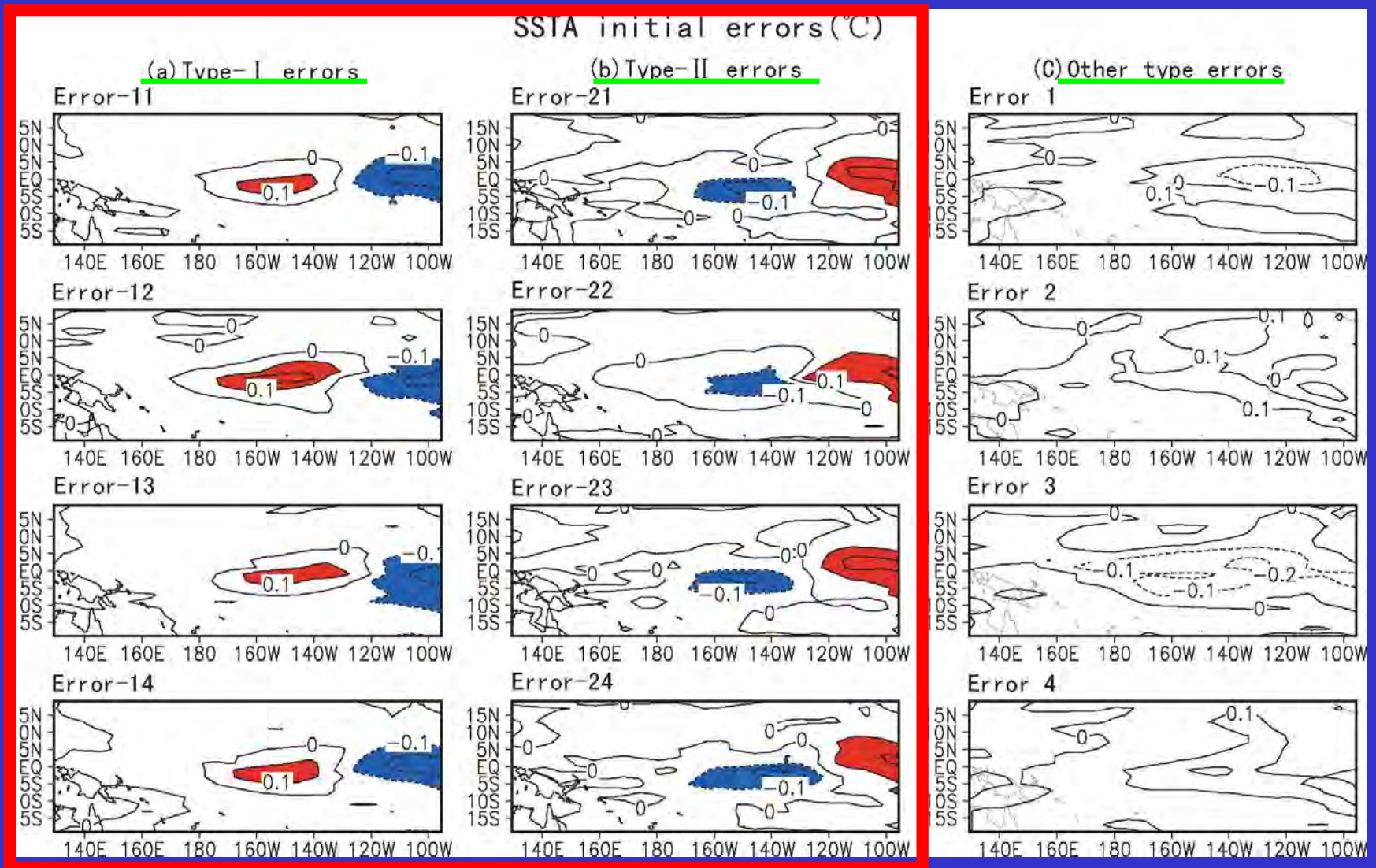
The initial errors that cause a significant SPB can be divided into two types: **one type (type-I) causes a negative prediction error of Nino-3 SSTA; the other (type-II) causes a positive prediction error.** In the table are eight representatives of the initial errors.

**For the strong El Nino with initial warming time January**

**Table 4. Seasonal growth rates of Type-I and -II errors for the strong El Niño with initial warm in January**

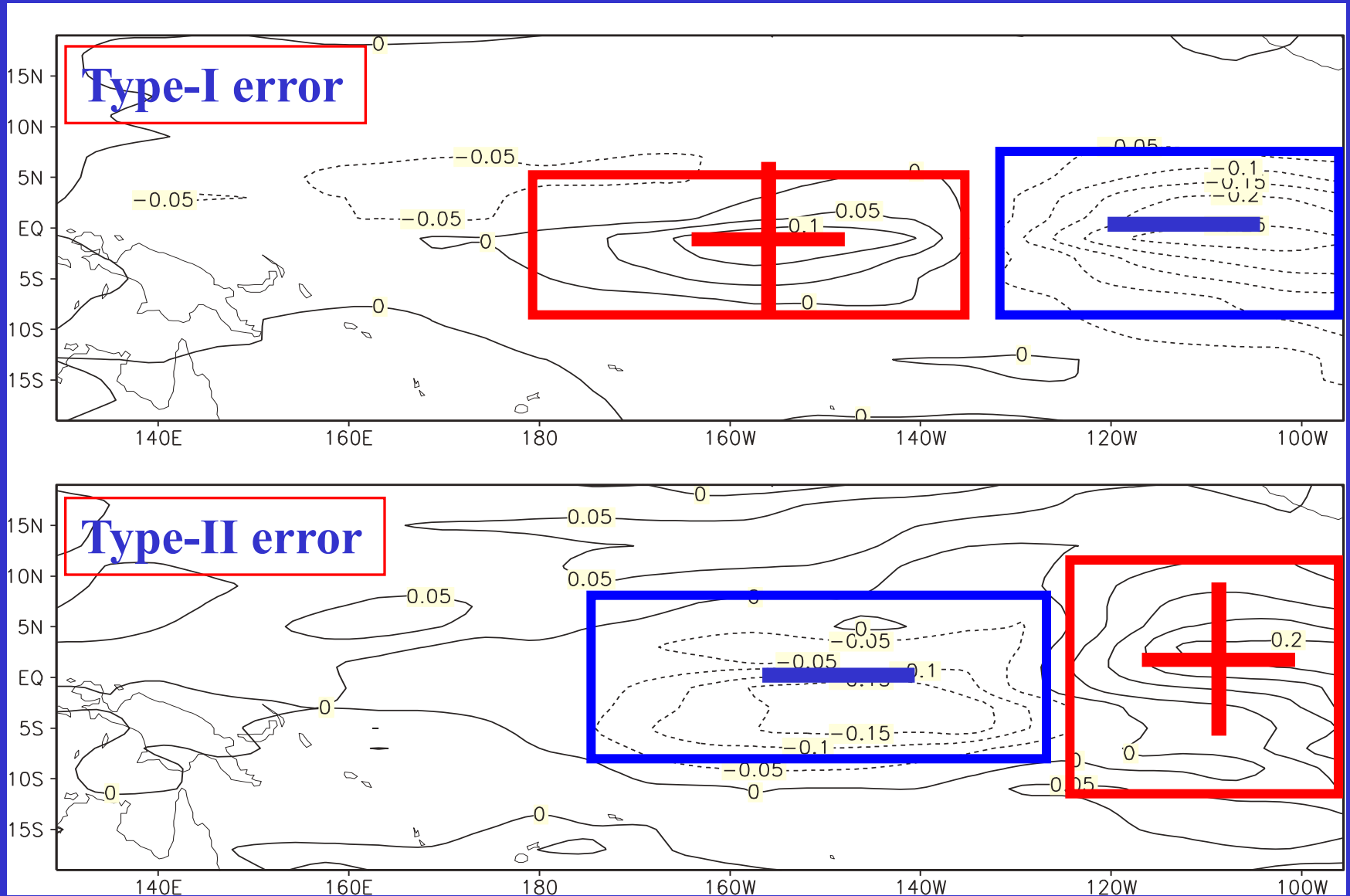
SSTA errors	JFM	AMJ	JAS	OND	$E_{Nino-3}$
Error – 11	0.246	<b>2.609</b>	<b>2.759</b>	-1.501	-0.306
Error – 12	0.410	<b>3.437</b>	<b>3.936</b>	-1.167	-0.549
Error – 13	0.109	<b>2.509</b>	<b>3.511</b>	-0.861	-0.428
Error – 14	-0.177	<b>2.229</b>	<b>4.236</b>	-0.128	-0.561
Error – 21	-0.072	<b>1.771</b>	<b>2.576</b>	-1.384	0.126
Error – 22	0.098	<b>1.647</b>	<b>2.251</b>	-1.311	0.105
Error – 23	-0.032	<b>1.857</b>	<b>2.424</b>	-1.398	0.115
Error – 24	-0.219	<b>1.747</b>	<b>3.312</b>	-1.267	0.171

# Representatives of Type-I and Type-II errors for strong El Nino



There are other types of errors that yield a less significant SPB or do not cause a SPB.

# Composite of SSTA component of type-I and -II errors for 20 strong El Nino events



## For the weak El Nino with initial warming time October

Table 3. Seasonal growth rates of Type-I and -II errors for the weak El Niño with initial warm in October

SSTA error	OND	JFM	AMJ	JAS	$E_{Nino-3}$
Error - 11	0.020	0.964	<b>2.355</b>	0.975	-0.452
Error - 12	0.389	1.234	<b>2.947</b>	0.764	-0.511
Error - 13	-0.109	0.913	<b>2.856</b>	1.171	-0.477
Error - 14	-0.058	0.899	<b>2.436</b>	1.046	-0.458
Error - 21	-0.035	0.630	<b>2.898</b>	2.143	0.493
Error - 22	-0.050	0.774	<b>2.503</b>	1.728	0.533
Error - 23	-0.286	0.514	<b>2.317</b>	1.532	0.449
Error - 24	-0.001	0.704	<b>2.929</b>	1.938	0.574

The initial error that cause a significant SPB for weak El Nino events can also be classified into two types.

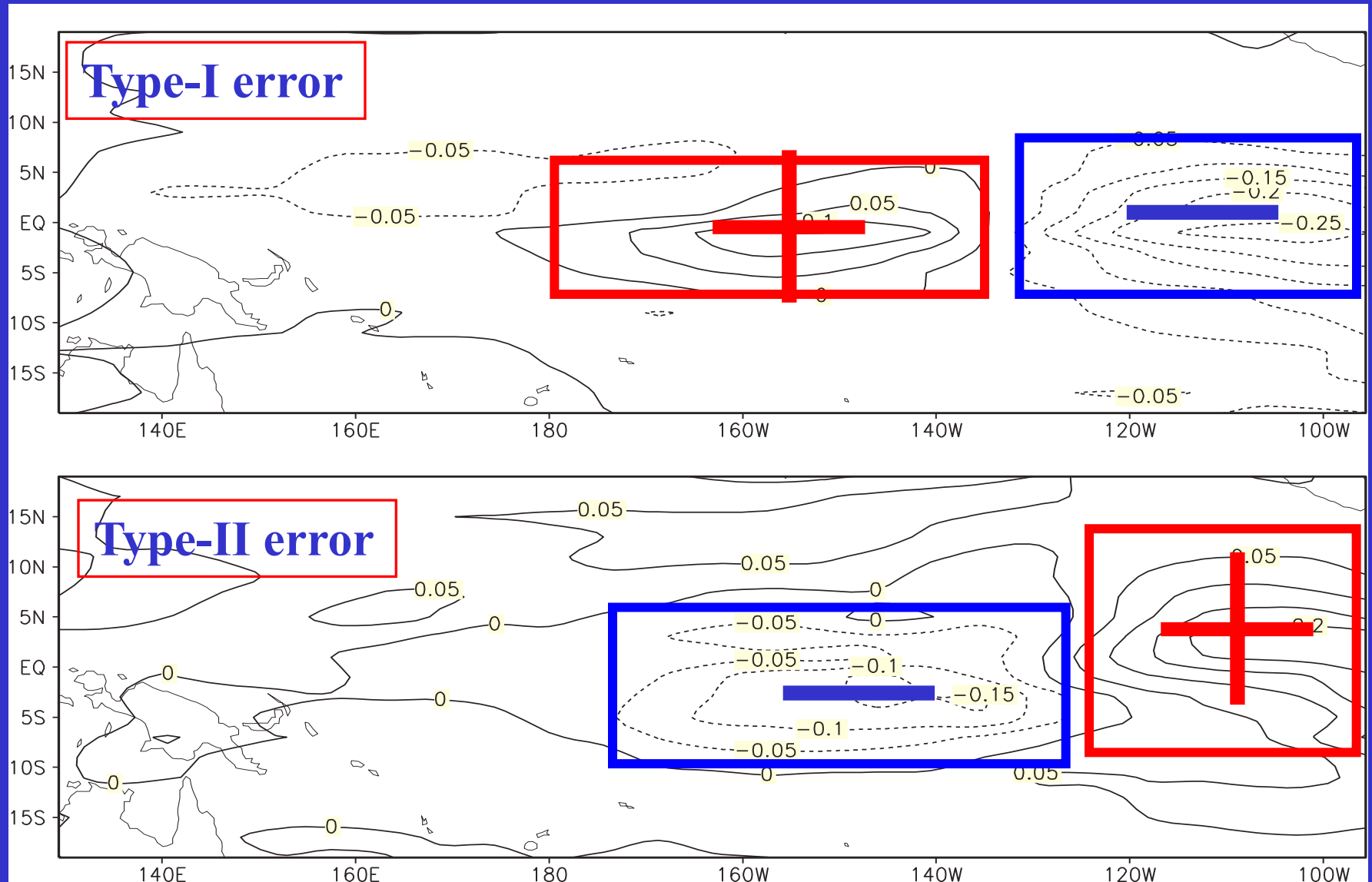
## For the weak El Nino with initial warming time January

Table 5. Seasonal growth rates of Type-I and -II errors for the weak El Niño with initial warm in January

SSTA errors	JFM	AMJ	JAS	OND	$E_{Nino-3}$
Error - 11	0.472	<b>4.006</b>	<b>4.498</b>	-0.591	-0.860
Error - 12	0.580	<b>4.691</b>	<b>4.680</b>	-1.613	-0.856
Error - 13	0.305	<b>4.129</b>	<b>5.078</b>	-0.527	-0.905
Error - 14	0.411	<b>4.029</b>	<b>4.614</b>	-0.634	-0.861
Error - 21	0.078	<b>2.651</b>	<b>3.499</b>	0.569	0.719
Error - 22	0.048	<b>2.911</b>	<b>4.975</b>	1.743	0.983
Error - 23	-0.107	<b>2.501</b>	<b>4.208</b>	1.227	0.822
Error - 24	0.087	<b>2.844</b>	<b>4.348</b>	1.206	0.872

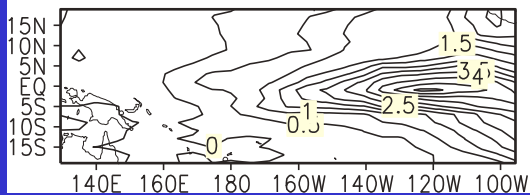
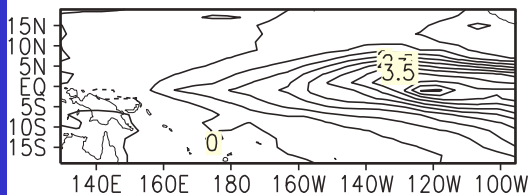
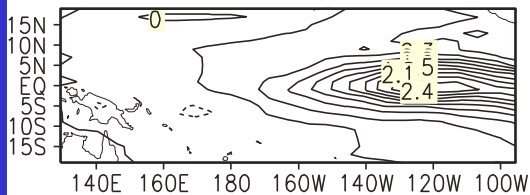
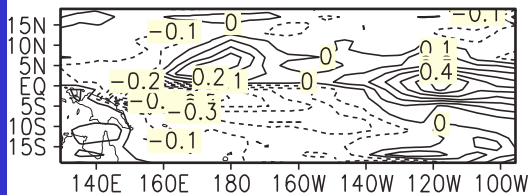
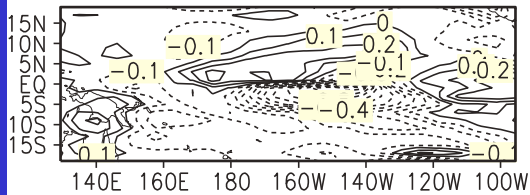
The initial error that cause a significant SPB for weak El Nino events can also be classified into two types.

# Composite of SSTA of type-I and -II errors for 40 El Nino events (including 20 strong ones and 20 weak ones)

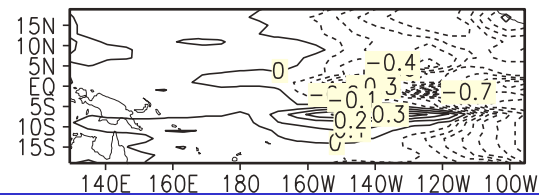
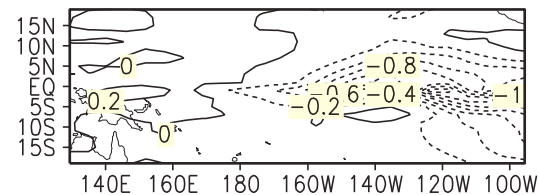
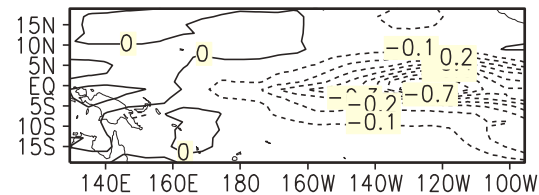
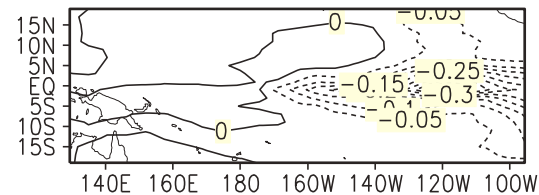
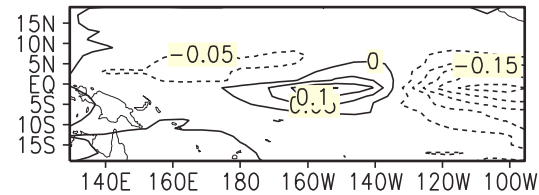


# Evolutions of El Nino, type-I and type-II errors

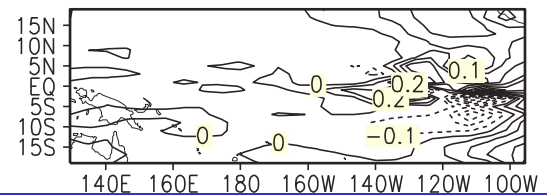
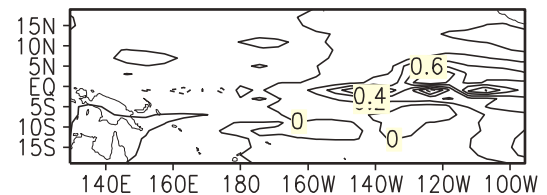
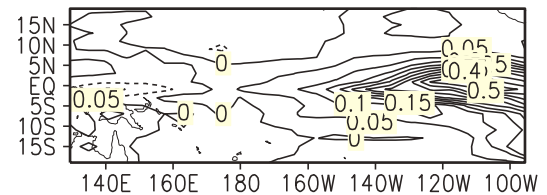
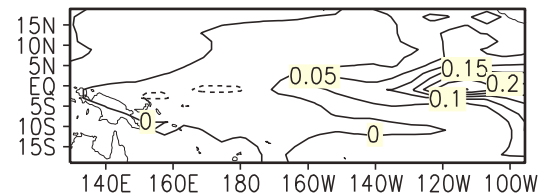
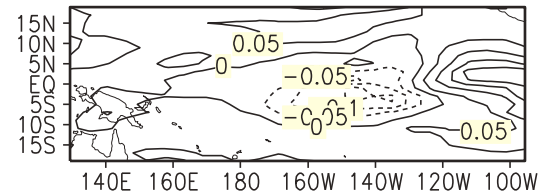
## Evolution of El Nino



## Evolution of type-I error



## Evolution of type-II error



**El Nino-Southern Oscillation (ENSO):** a prominent climate phenomenon in the coupled ocean-atmospheric system of tropical Pacific

**Significant progresses in ENSO theory and prediction**  
*(Tropical Ocean Global Atmosphere; TOGA program)*

*Walker 1924; Bjerknes, 1969; Zebiak and Cane, 1987; Webster and Yang, 1992; Chen et al., 1996; Moore and Kleeman, 1996; Jin et al., 1997; Neelin et al., 1998; Wang, 2001; Samlson and Tziperman, 2002; An and Jin, 2004; Mu et al., 2007a,b; Duan et al., 2006;2008;2009; Tang et al., 2008;*

*.....and so on*

## **A significant SPB**

**From the perspective of error growth, a significant SPB can be characterized by two aspects:**

**(1) the ENSO forecasting has a large prediction error;**

**in particular,**

**(2) a prominent error growth occurs in the spring when the predictions are made before the spring, that is, a season-dependent evolution of the prediction errors.**

*(Mu et al., 2007a,b; Duan et al., 2009; Yu et al., 2009).*

### 3. Seasonal growth rate of the prediction errors caused by the combined mode of CNOP-I and CNOP-P errors

Growth-phase predictions

Start month: July in year(-1)

Large prediction errors

El Nino	JAS	OND	JFM	AMJ	$E_{Ni\tilde{n}o-3}$
WR <sub>1</sub>	0.852	1.39	3.966	1.75	-0.996
WR <sub>2</sub>	1.854	2.935	-0.38	8.084	2.527
WR <sub>3</sub>	2.197	3.238	1.823	3.665	2.032
WR <sub>4</sub>	2.52	3.535	2.031	3.411	2.056
SR <sub>1</sub>	1.317	1.53	3.672	4.689	-1.874
SR <sub>2</sub>	0.921	0.613	1.607	5.051	-1.512
SR <sub>3</sub>	2.013	3.077	3.52	5.432	-2.214
SR <sub>4</sub>	1.914	2.918	0.855	0.711	1.072

Start month: October in year(-1)

Large prediction errors

El Nino	OND	JFM	AMJ	JAS	$E_{Ni\tilde{n}o-3}$
WR <sub>1</sub>	0.874	2.046	5.662	7.826	3.015
WR <sub>2</sub>	1.276	1.159	5.92	9.249	3.273
WR <sub>3</sub>	1.499	1.806	4.789	5.048	2.485
WR <sub>4</sub>	1.126	1.721	4.428	3.928	1.992
SR <sub>1</sub>	1.891	3.342	7.508	3.561	-2.827
SR <sub>2</sub>	0.966	1.575	5.724	7.39	-2.95
SR <sub>3</sub>	1.578	2.484	5.907	3.289	-2.209
SR <sub>4</sub>	1.271	1.813	4.74	4.099	-2.063

Large prediction errors

Start month: January in year(0)

El Nino	JFM	AMJ	JAS	OND	$E_{Ni\tilde{n}o-3}$
WR <sub>1</sub>	1.013	4.581	8.407	2.589	3.056
WR <sub>2</sub>	1.038	3.165	4.637	4.077	-2.356
WR <sub>3</sub>	1.098	4.801	6.395	1.336	2.445
WR <sub>4</sub>	0.787	3.091	5.672	2.406	-2.19
SR <sub>1</sub>	0.958	5.327	7.054	0.762	-2.501
SR <sub>2</sub>	1.215	3.434	6.835	4.573	-2.991
SR <sub>3</sub>	1.408	4.276	6.907	2.996	-2.828
SR <sub>4</sub>	1.667	4.196	7.09	2.68	-2.776

For the growth-phase predictions, the combined mode of CNOP-I and CNOP-P errors have **obvious season-dependent evolutions**. Furthermore, they cause **a large prediction error**.

The decaying-phase predictions have similar results.

The combined mode causes a significant SPB.

Many works have investigated the SPB for ENSO events.

## Debates remain concerning

### (i) its causes:

The weakest zonal SST gradient during spring (*Webster and Yang, 1992; Lau and Yang, 1996*).

The weakest ocean-atmosphere coupling during spring (*Webster, 1995*)

Small SST signals in spring (*Chen et al., 1995*)

..... *and so on.*

**There is an urgent need to further address the problems related to the SPB for ENSO events.**

**Understanding of SPB can be gained by studying the initial error growth** *(Moore and Kleeman, 1996; Samelson and Tziperman, 2001; Mu et al., 2007a, b).*

# The prediction uncertainties: **initial errors and model errors.**

## Questions:

1. Can initial errors cause a significant SPB ?
2. How about model errors? . **Which kind of errors play the dominant role in yielding a significant SPB, initial errors or model errors?**

# Decadal variation of THC

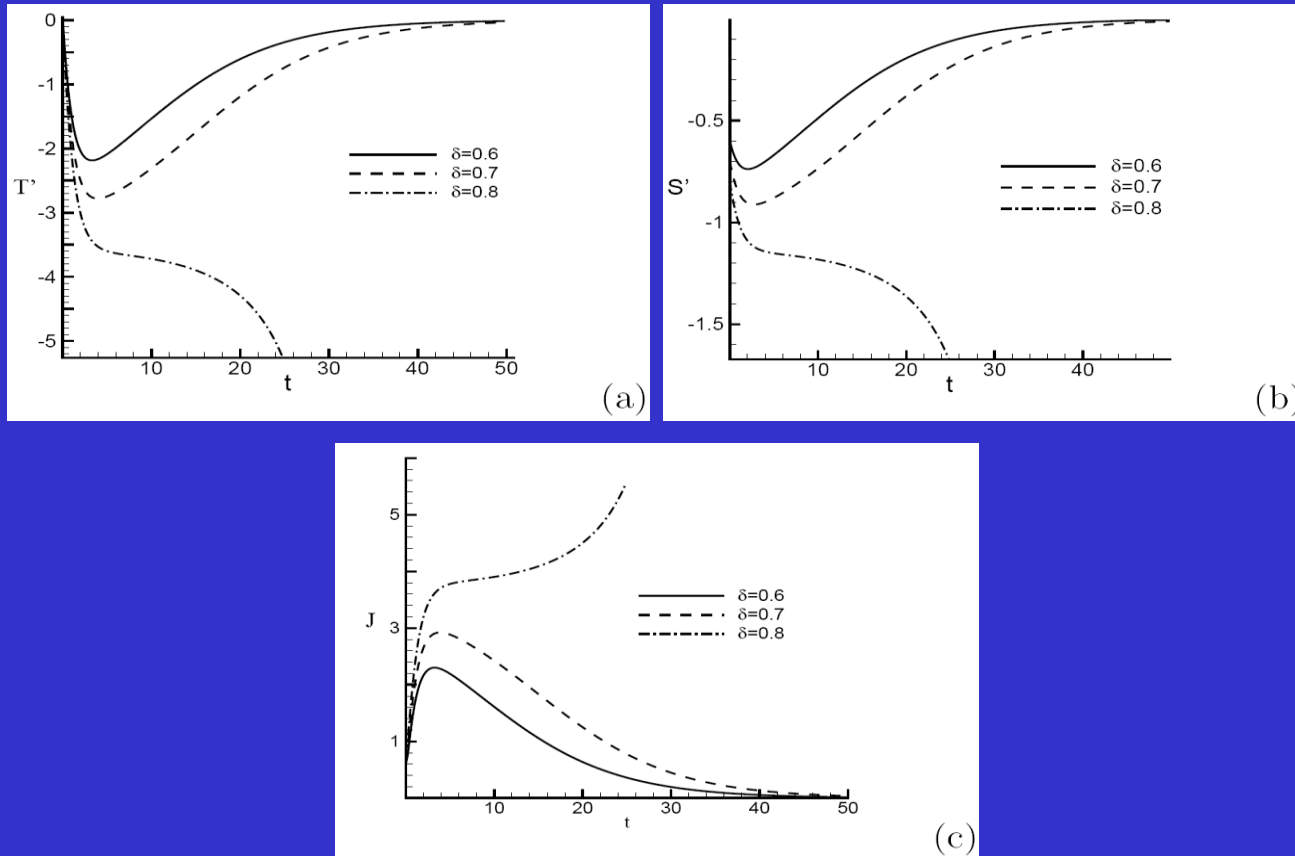
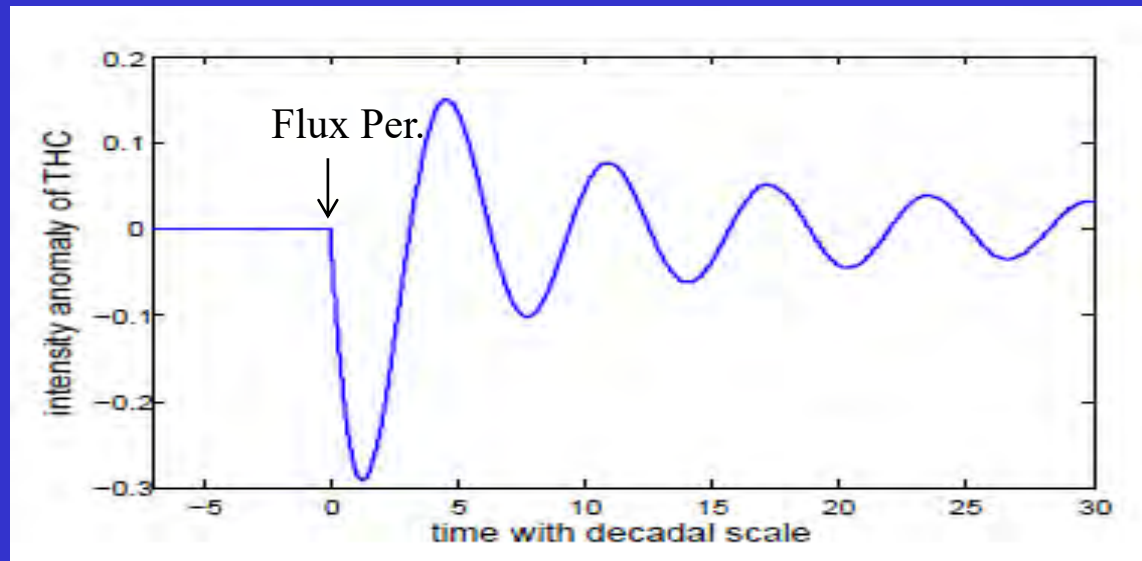


Figure 7: The evolution of (a) temperature  $T'$ , (b) salinity  $S'$ , (c) magnitude  $J$  of CNOPs. The solid, dashed, dash dotted curve represent  $\delta = 0.6, 0.7,$  and  $0.8,$  respectively.

- **In our work, we suppose that external forcing (fresh water or heat flux) changes the variables( SST or Sea Surface Salinity: SSS) of the ocean from the steady state, while it's the recovery processes of these variables that causes decadal variability of THC.**



**We employed two models, a simple box model and a 3D ocean general circulation model.**

## 4.2 Results of OGCM:

### Model and its configuration

- 1 THCM: a 3D ocean general circulation model, which is a fully implicit model and can produce the tangent linear and adjoint matrix.
- 2 Domain: [286W, 350W] \* [10N, 74N]; without geometry.
- 3 Resolution: 4° \* 4° \* 250m
- 4 Uniform basin depth: 4000m
- 5 Time step: from 0.7-14 days

### Restoring Boundary for T and S

$$F_T^R = \frac{SST_p - SST}{\tau_T}; F_S^R = \frac{SSS_p - SSS}{\tau_S}$$

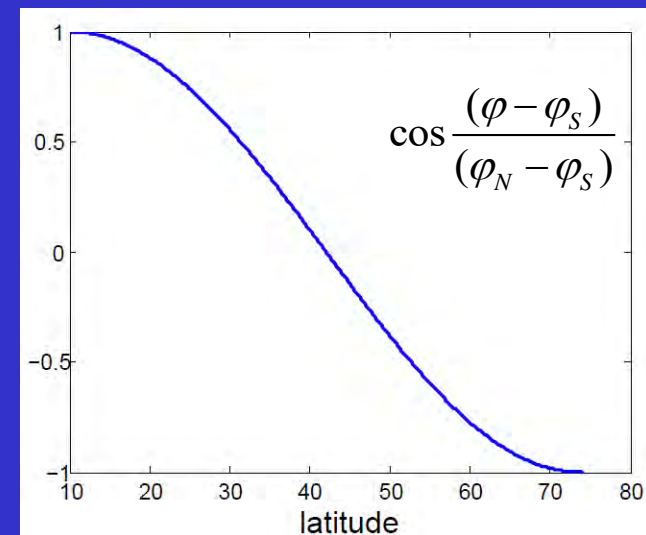
$SST_p, SSS_p$  are the prescribed SST and SSS, and  $\tau_T, \tau_S$  are restoring scales of SST and SSS, respectively.

$$SST_p(\varphi) = A \cos \frac{(\varphi - \varphi_S)}{(\varphi_N - \varphi_S)}; SSS_p(\varphi) = B \cos \frac{(\varphi - \varphi_S)}{(\varphi_N - \varphi_S)}$$

After the model reaches the steady state, switch to flux boundary.

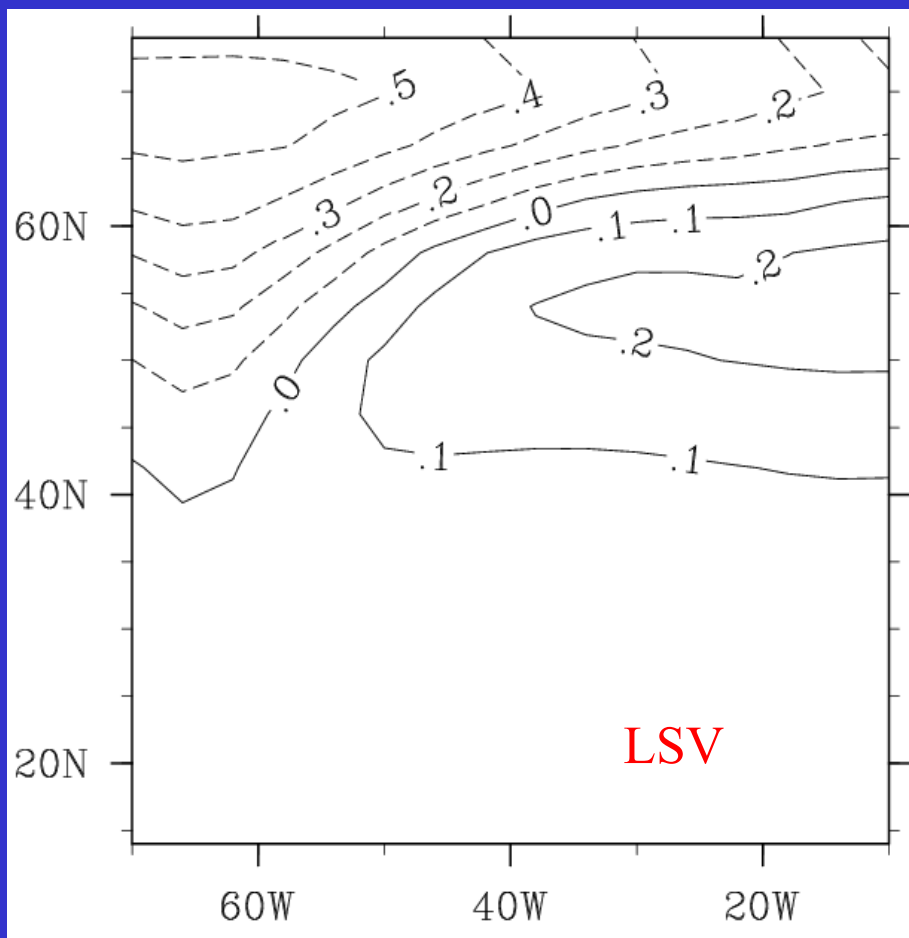
$$F_T^F = F_T^R; F_S^F = F_S^R$$

Without wind forcing



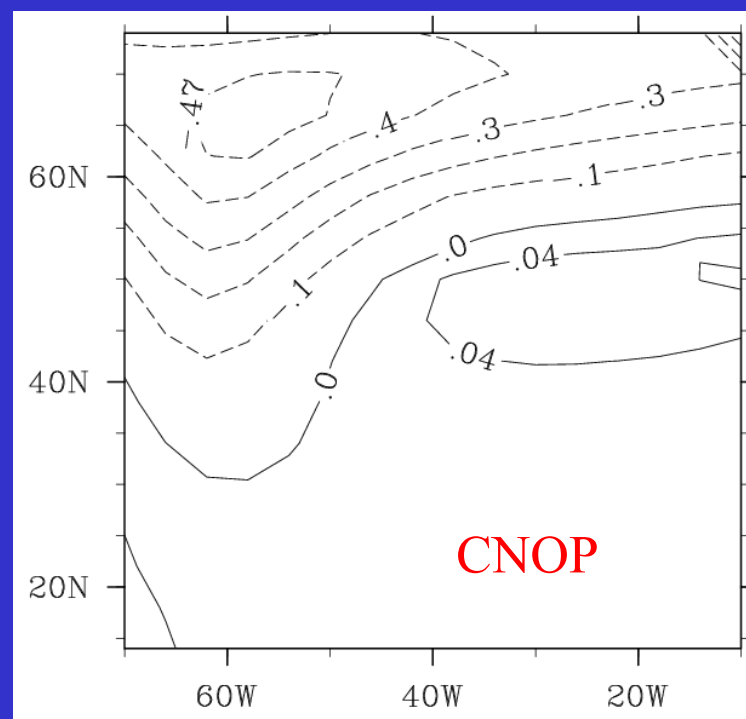
# Optimal initial SSS perturbations by LSV

To compare with the previous work, we obtained the optimal perturbations by LSV. The configuration of LSV is the same with that of CNOP, except the nonlinear model is replaced by tangent linear model.

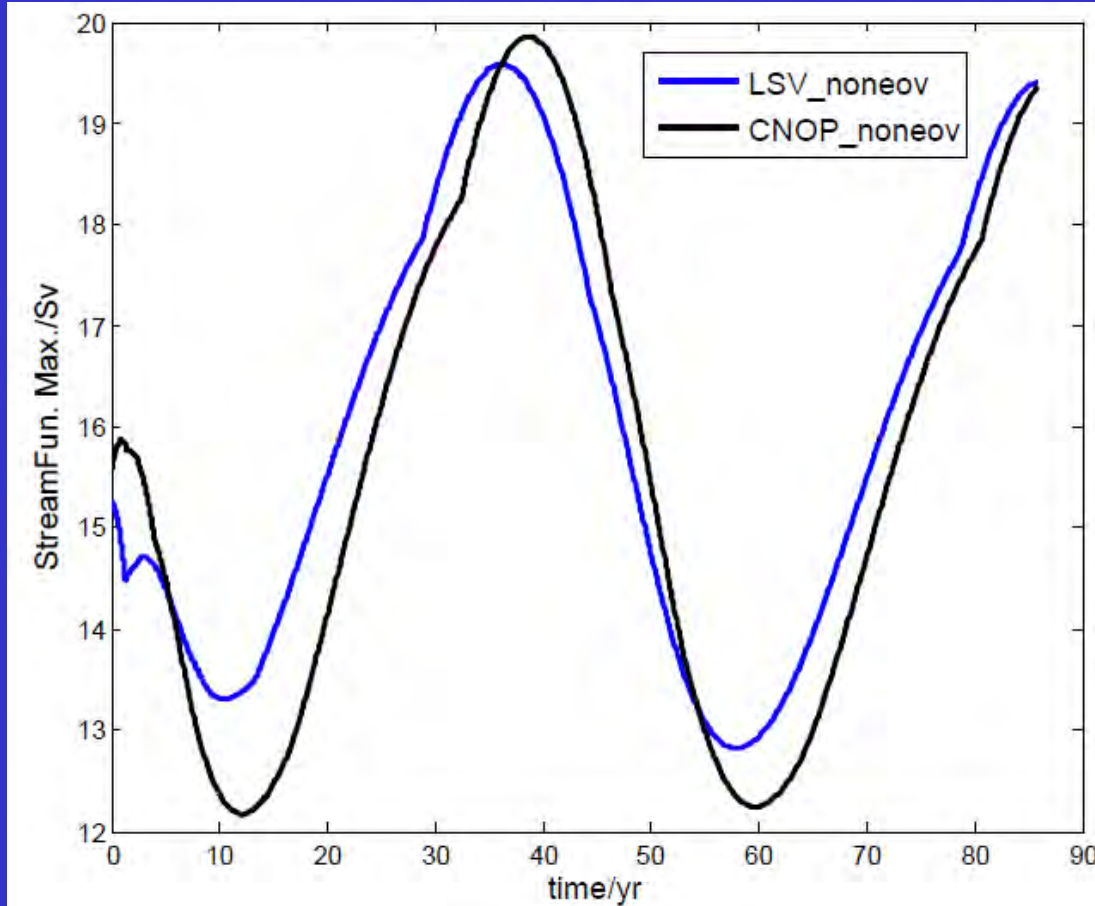


unit: psu

Perturbations obtained by LSV are similar to those by CNOP, except a stronger westward extending of positive perturbations in the mid-latitude.



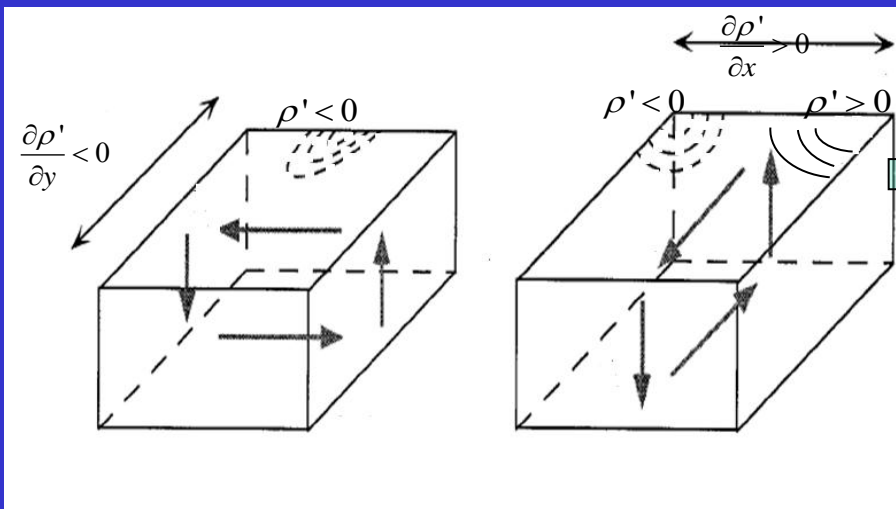
# Variations induced by initial perturbations



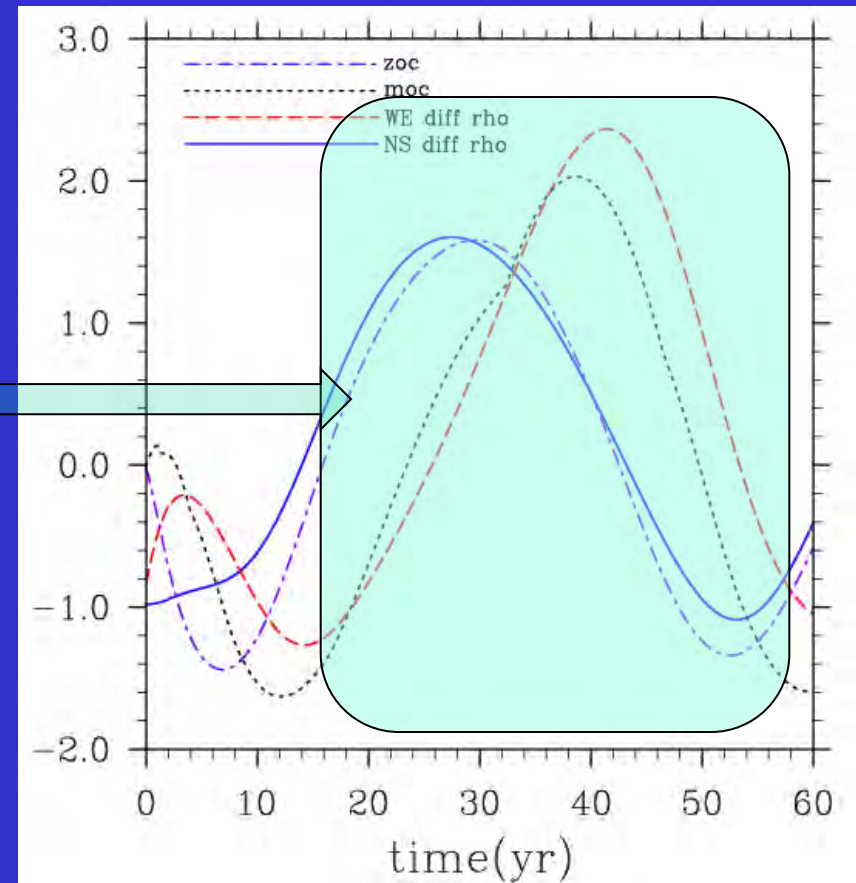
Compared to the perturbations by LSV, those by CNOP can induce stronger decadal variations of THC, that is, stronger negative anomalies (about 1 Sv) of streamfunction maximum in the negative phase and stronger positive anomalies (about 0.2 Sv) in the positive phase.

# The physics of oscillation

## Thermal wind relation



Modified from Raa and Dijkstra, 2002



These four indices have been standardized

# The Mechanism of Nonlinear Feedback For Thermohaline Circulation

The evolution equation of  $\psi' = \langle \mathbf{b}, \mathbf{x} \rangle$

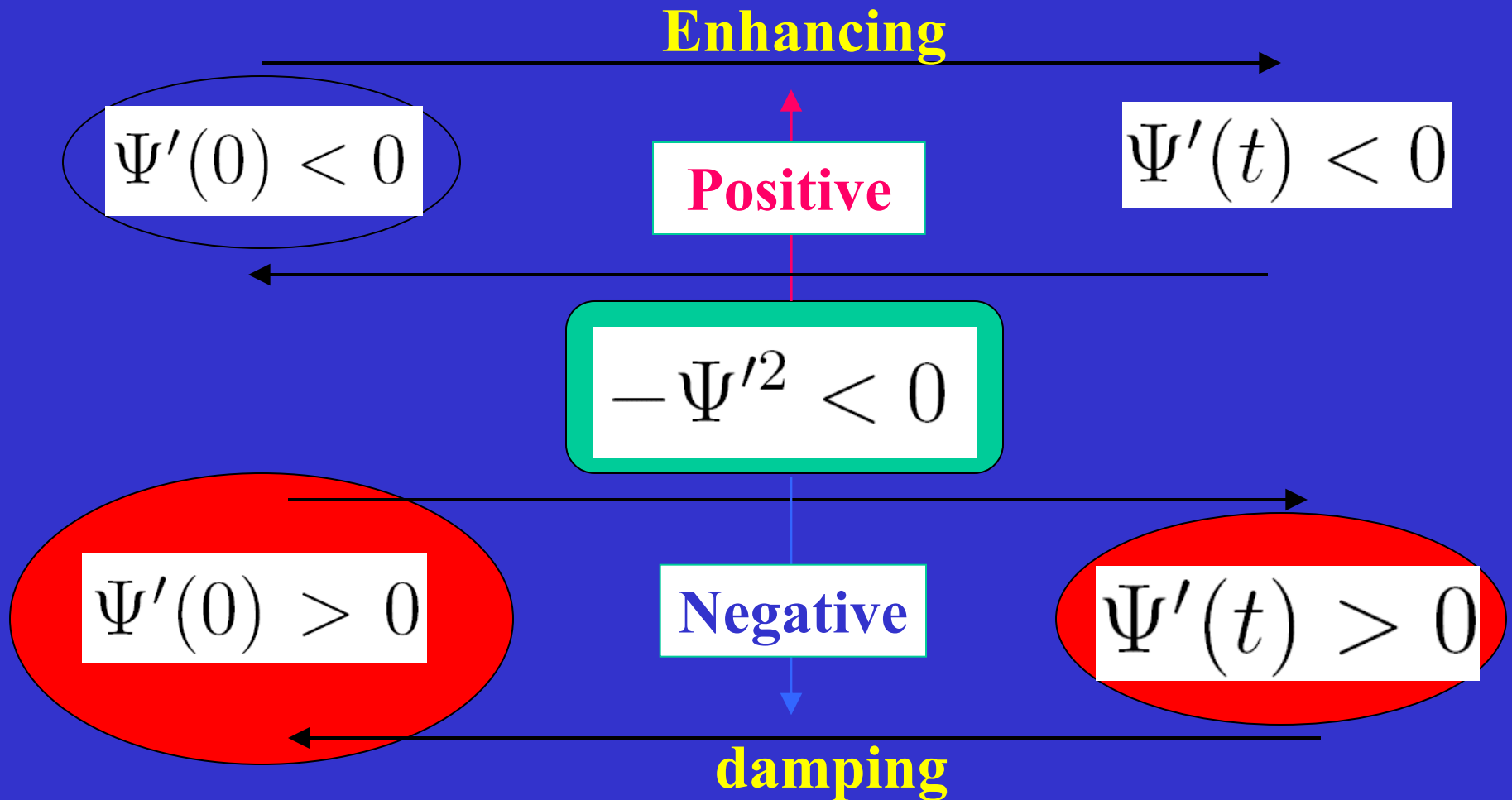
$$\frac{d}{dt} \psi' = \langle \mathbf{b}, \mathbf{A}\mathbf{x} \rangle - \psi'^2 \quad (4)$$

Integrating the above equation, we find

$$\psi'(t) = \psi'(0) + \int_0^t L(\mathbf{x}) d\tau - \int_0^t \psi'^2 d\tau \quad (5)$$

where  $L(\mathbf{x}) = \langle \mathbf{b}, \mathbf{A}\mathbf{x} \rangle$

# Nonlinear Feedback (TH)



# Predictability is a fundamental issue in Weather and climate prediction

**What is the predictability? Not a unified definition.**

**Predictability study: the uncertainty of forecast results  
(Mu et al., 2004)**

- (i) The analysis of the factors and mechanisms that yield these uncertainties**
- (ii) The search for methods and approaches to reduce these uncertainties.**